REPORT DOCUMENTATION PAGE

Public reporting burden for this collection of information is estimated to average 1 hour per response, including the time for reviewing instructions, searching existing data sources, gathering and maintaini needed, and completing and reviewing the collection of information. Send comments regarding this burden estimate or any other aspect of this collection of information, including suggestions for reducing th Washington Headquarters Services, Directorate for Information Operations and Reports, 1215 Jefferson Davis Highway, Suite 1204, Arlington, VA 22202-4302, and to the Office of Management and Budget Reduction Project (0704-0188) Washington, DC 20503.

1. AGENCY USE ONLY (Leave blank)	2. REPORT DATE 25 APRIL 97	3. REPORT TYPE AND DATES COVERED FINAL REPORT 01/01/93 - 01/19/96

4. TITLE AND SUBTITLE Semiconductor Ultraviolet Detectors	5. FUNDING NUMBERS N/N00014-93-1-0241

6. AUTHOR(S)

P. I. Cohen and M. I. Nathan

7. PERFORMING ORGANIZATION NAME(S) AND ADDRESS(S) Dept. of Electrical Engineering University of Minnesota 200 Union Street SE Minneapolis, MN 55455	8. PERFORMING ORGANIZATION REPORT NUMBER

9. SPONSORING/MONITORING AGENCY NAMES(S) AND ADDRESS(ES) Office of Naval Research Code 312, Room 607 800 Quincy St. Arlington, VA 22217-5660	10. SPONSORING/MONITORING AGENCY REPORT NUMBER

11. SUPPLEMENTARY NOTES

12a. DISTRIBUTION/AVAILABILITY STATEMENT Approved for public release; distribution unlimited.	12b. DISTRIBUTION CODE

13. ABSTRACT (Maximum 200 words)

Materials and structures crucial to the development of semiconducting ultraviolet detectors were examined. The chemical beam epitaxy of GaN was compared to the growth of GaN using supersonic jet sources. The main characterization techniques employed were reflection high energy electron diffraction (RHEED) and desorption mass spectroscopy (DMS). It was found that a supersonic jet of molecular nitrogen seeded in molecular hydrogen would react at the surface to form GaN at incident energies exceeding 6.7 ev. The growth was compared to that from a supersonic jet of ammonia and a conventional ammonia leak. It was found that higher fluxes could be obtained using the ammonia leak. No differences in the growth were found using the ammonia jet. Using DMS it was found, however, that the jet assisted adsorption had different kinetics vs surface coverage than the ammonia adsorption. For the growth with ammonia, DMS and RHEED were used to establish a framework for the growth of GaN. This framework allows one to reproduceably set growth conditions and predict rates. Finally Schottky barrier heights were measured and DX-like centers examined vs hydrostatic pressures.

14. SUBJECT TERMS GaN, Epitaxy, Supersonic Jet, Ammonia	15. NUMBER OF PAGES
	16. PRICE CODE

17. SECURITY CLASSIFICATION OF REPORT UNCLASSIFIED	18. SECURITY CLASSIFICATION OF THIS PAGE UNCLASSIFIED	19. SECURITY CLASSIFICATION OF ABSTRACT UNCLASSIFIED	20. LIMITATION OF ABSTRACT Unlimited

NSN 7540-01-280-5500

19970502 181

DTIC QUALITY INSPECTED 4

Contents

1 Introduction

Three main efforts were initiated under this program entitled "Semiconductor Ultraviolet Detectors:"

- Evaluate the growth of GaN using a supersonic jet

- Develop structures for UV detectors

- Evaluate the growth of GaN using ammonia

These relied on the development of supersonic sources of nitrogen and ammonia as well as the installation and conversion of a Varian GenII molecular beam apparatus. Hiqh quality GaN films were grown, supersonic jet sources studied, and a basic growth kinetics using ammonia established. This last was the most successful, leading to the development of a fundamental framework for the growth of GaN. With this framework one can now reproduceably set growth conditions. Using this framework we are now studying the microscopic growth mechanisms of (Al,In,Ga)N. The first effort led to the construction of a high temperature supersonic jet of nitrogen seeded in hydrogen. Using desorption mass spectroscopy we found that the incident translational energy provided by the jet was sufficient to enable the use of molecular nitrogen for the growth of GaN and that the growth kinetics were different than with ammonia. However, the design of the MBE apparatus precluded attaining high fluxes needed for film growth at reasonable rates. Finally, the Schottky barriers in detector structures were measured for Pt/GaN and Pd/GAN and a DX-like center was examined vs hydrostatic pressure.

2 Final Technical Report

2.1 RHEED Intensity Oscillations

Following reports by Yoshida and Wang, RHEED intensity oscillations measurements of RHEED intensity oscillations were attempted. Surprisingly, these were not observed and the information reported in these two papers were insufficient to reproduce the effect. Ultimately, Johnston was able to show that, the growth conditions, the starting buffer, and the film preparation procedures were all crucial. He found for example that AlN starting buffers did not yield RHEED intensity oscillations; by contrast, GaN buffers did. Currently we are examining the differences in these two surfaces, with the suspicion that they are related to differences in the orientation (A or B) of the GaN grown on our sapphire substrate. Alternatively,

the density of inversion domains might be different. These conditions are currently being described in an invited review comparing N vs Ga limited growth modes.

Yoshida claimed that the period of the intensity oscillations they observed during the growth of GaN corresponded to the growth rate. Our measurements indicate that this is not so, but that the period depends on the N flux and on the surface preparation. Though the period is linear with Ga flux, it does not extrapolate to zero in the limit of zero Ga flux. This offset is sensitive to the ammonia flux. As yet no obvious surface defect has been identified as the modification in the growth period.

Using the intensity oscillations at temperatures as low as about 500°C, we were able to show that ammonia dissociates at the surface even at low temperatures, though the rate is somewhat decreased. At higher temperatures there are no barriers to ammonia dissociation as long as there is Ga terminated GaN accessible to it.

2.2 Supersonic Jets

A main goal of this research was to determine whether translational kinetic energy given to nitrogen molecules would enable the molecule to surmount a dissociation barrier and chemisorb. The expectation was that the collision of the molecule and surface would cause a change in the molecular bonding geometry, weakening bonds and allowing dissociation. Our goal was to determine whether a supersonic expansion could provide this additional kinetic energy. Being a very strongly bonded molecule, we expected that exceedingly high incident energies would be required to cause molecular nitrogen to react at the GaN surface. As a result a supersonic jet was constructed that could reach near the melting point of W. This jet consists of a resistively heated tube with a small aperture on the side. A drawing is shown in Fig. 1. The end connections are water cooled and power is provided along the same lines as the water cooling. The nitrogen is seeded in a largely hydrogen mixture. By heating to high temperature, the hydrogen is given a large kinetic energy by virtue of its small mass. Momentum exchange forces the smaller concentration of nitrogen molecules along at the same velocity, but with a larger kinetic energy.

The role of the additional kinetic energy was examined using desorption mass spectroscopy to monitor the chemical reactions at the GaN surface. Fig. 2 and 3 show measurements of Ga desorbed from a GaN surface without and with a nitride layer present. The main idea is to measure the amount of Ga that can adsorb if a surface was previously nitrided using a supersonic jet. The data show that the nitrogen kinetic energy needs to be about 6.7 eV before dissociative chemisorption occurs.

Data taken for two different incident energies (nozzle temperatures) are presented. The method is as follows: For a substrate at a given temperature and in the absence of a nitrogen source, Ga will adsorb until a steady state surface coverage is reached. At that point the desorption flux equals the incident flux. This will give rise to a linear increase in surface Ga coverage unless there is a reaction that forms GaN. In the latter case one expects the adsorbed Ga to react; then after a short time all will be reacted and the coverage of Ga will build up until steady state is reached. In the curves here, this delay in the desorption curve is only apparent for the high temperature curve in Fig. 3. For Fig. 2, where the surface was not previously exposed to the nitrogen jet, there is no delay. Using this titration we determine that a nozzle temperature of 2500°C is required for dissociative chemisorption. For the mix of N_2/H_2 that was used, this corresponds to an incident translational energy of about 6.7 eV.

These data were compared to those obtained using an ammonia jet and to an ammonia leak. The detailed uptake of Ga was different, suggesting that the structure formed on the surface was different. At this point we do not know what those differences are due to and do not have funding to investigate it. The ammonia jet behaved in most respects as the ammonia leak. There was additional reactivity due to the increased translational energy – likely because the ammonia was reactive enough to adsorb when there were reactive Ga sites available. Its jet action served to increase the flux vs ammonia useage, but the advantage was minimal since at the high ammonia fluxes desired the jet could not be maintained.

The main conclusion from this work that molecular nitrogen could be given sufficient translational energy to dissociatively adsorb. Insufficient work was done to determine the differences in the nitrided surface formed from the N_2/H_2 jet vs an ammonia leak. Because of the flux differential it was concluded that pursuit of growth with the N_2/H_2 jet was not a promising avenue for research.
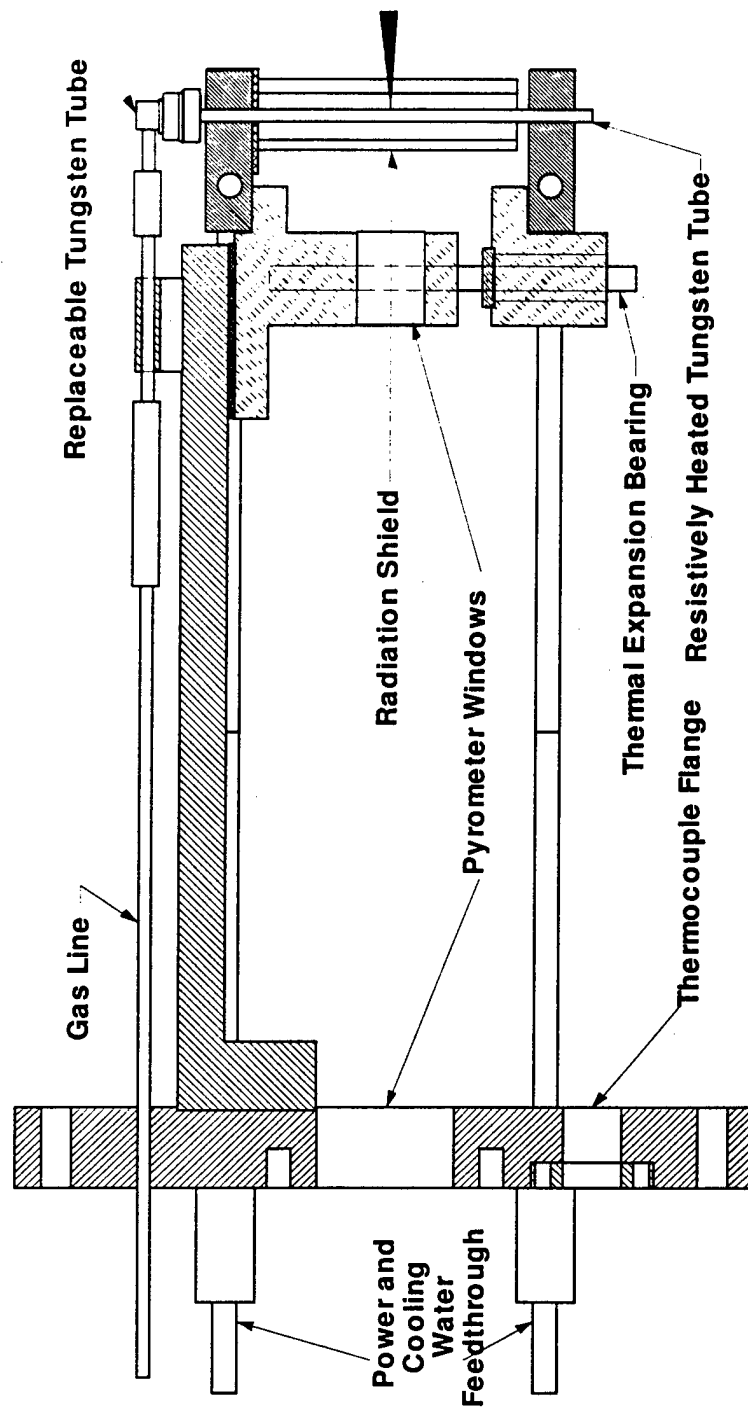
Figure 1: Drawing of the high temperature supersonic jet. Gas emerges at the arrow at the top from a small hole in a directly heated W tube.
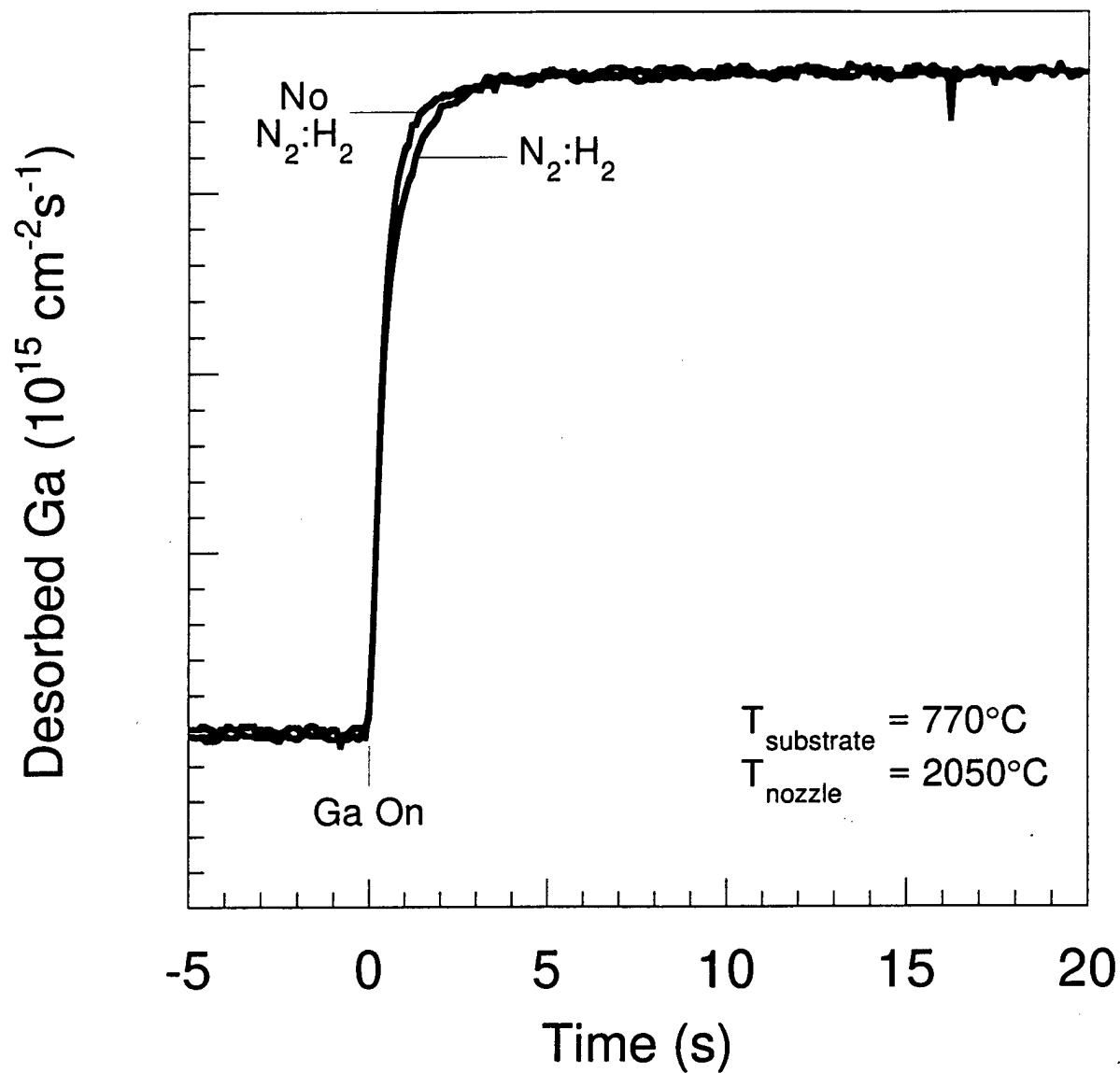
Figure 2: DMS measurement of Ga desorbed from a GaN surface after the initiation of a Ga flux. There is little difference between a surface that has not been nitrided and a surface that has been exposed to a nitrogen/hydrogen jet at 2050°C. We interpret this as at this incident energy there is no dissociation.
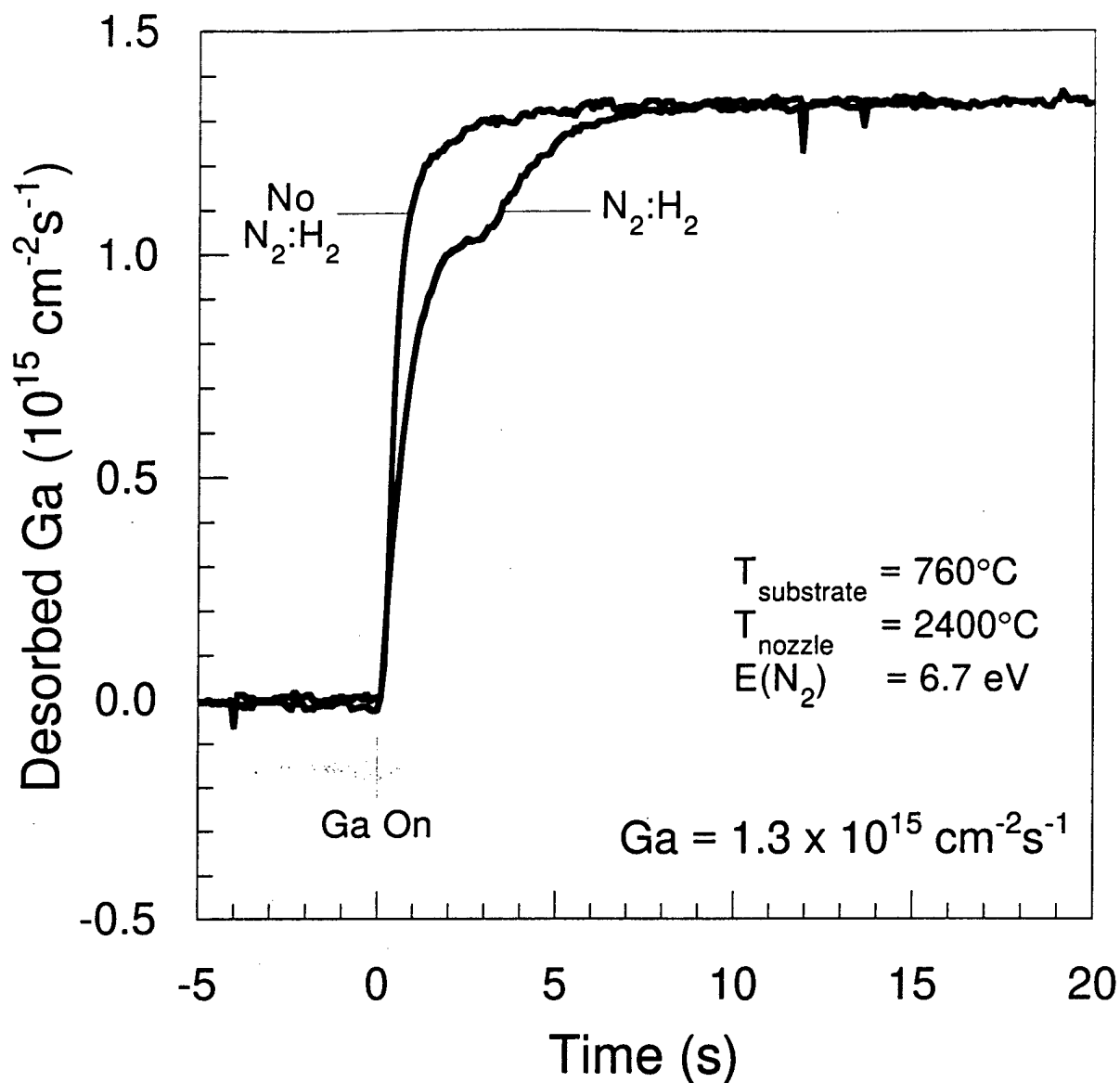
6

Figure 3: DMS measurement of Ga desorbed from a GaN surface after the initiation of a Ga flux. In one case the surface has not been nitrided; in the other it has been exposed to a high energy molecular nitrogen flux. There is chemisorption of Ga, indicating that about 6.7 eV is required to dissociate molecular nitrogen on GaN.

2.3

Growth Rate Reduction of GaN Due to Ga Surface Accumulation

Devin Crawford, Ruediger Held, A. M. Johnston, A. M. Dabiran, Philip I. Cohen
Department of Electrical Engineering, University of Minnesota

Abstract

GaN(0001) has been grown on Al_2O_3 (0001) by molecular beam epitaxy where NH_3 was used as the nitrogen precursor. Desorption mass spectroscopy and reflection high energy electron diffraction (RHEED) were used to monitor the relationship between growth rate and the incident fluxes during growth. Excess surface Ga decreases the GaN formation rate when the substrate temperature is too low or the Ga flux is too high. A simple rate equation is used to describe the observed behavior.

1. Introduction

A number of issues related to growth kinetics of GaN must be addressed. Historically, the n-type conductivity commonly exhibited by GaN was attributed to N vacancies [1] . This problem was thought to arise from a kinetic barrier to N incorporation during growth. Recent results by Lee *et. al* [2] and also by Jones *et. al* [3] using NH_3 as the nitrogen precursor during molecular beam epitaxy (MBE) indicate that the GaN growth rate is strongly temperature dependent, exhibiting a maximum between 750°C and 800°C. The high temperature decrease in growth rate is typical of GaN, and has been attributed to Ga desorption at elevated substrate temperature [2] [3] as well as to the decomposition of GaN [4] . At lower substrate temperature the common belief is that reduced N incorporation efficiency limits the growth rate [2] .

In this paper we will address the low temperature issues related to GaN MBE where the GaN decomposition rate is much less than the growth rate . In section 3.1 we examine the transient response of the GaN surface composition and chemistry to a step-function of Ga flux. The time dependence of the Ga desorption after exposure of the surface to incident Ga indicates that Ga adsorbs to the surface in two states. The first deposited layer of Ga sticks to the surface in a strongly bound state, whereas subsequent desorption occurs at a higher rate. The more tightly bound of these layers is observed only when the surface has been previously exposed to NH_3.

In section 3.2 we examine the relationship between growth rate, substrate temperature and the incident fluxes. We show how desorption mass spectroscopy (DMS) can be used to determine whether the GaN formation rate is limited by the available N (Ga rich) or by the available Ga (N rich) and present a single rate equation to explain a decrease in the GaN formation rate with increasing Ga flux.

2. Experimental

Growth was carried out in a cryopumped Gen II MBE system which is shown schematically in Figure 1.

A quadrupole mass spectrometer mounted in one of the source ports enabled detection of the type and intensity of desorbed species from the substrate surface. The specular RHEED intensity was monitored using a photomultiplier tube. The NH_3 flux was held constant during growth using a capacitance manometer in conjunction with a closed loop PID controller and solenoid control valve to maintain constant pressure in the NH_3 gas line behind a manually regulated precision leak valve. A flux monitor located on the back of the sample manipulator was used to determine the incident beam equivalent pressure by rotating the sample manipulator. Absolute calibraiton of the incident Ga flux is achieved by monitoring RHEED intensity oscillations during growth of GaAs(001) in a separate experiment. Samples were prepared by successively cleaning in acetone and methanol, which was followed by a 5 minute etch at 70°C in 3:1 H_3PO_4:H_2SO_4. The substrates were then rinsed in deionized water and blown dry with N_2. This process resulted in atomically smooth surfaces that exhibited $\approx$ 1000 Å terraces as indicated by atomic force microscopy (AFM). Without the etch, AFM showed polish marks on the substrate surface, and no atomic steps could be seen.

The samples were loosely mounted via mechanical support in order to reduce thermal stress during growth. Consequently, thermal contact between the substrate heater and the sample was reduced, and a 0.2 μm layer of Ti was deposited on the back of the wafers to efficiently couple radiative energy from the heater to the substrate.

3. Results

3.1. Transient Response of the Surface Composition

The transient response of the specular RHEED intensity observed along the $<011\bar{2}>$ azimuth as well as the response of the desorbed Ga and H_2 fluxes to a step-function of incident Ga on the GaN surface are shown in Figure 2. These data were measured after growth had been terminated and the background NH_3 pressure had been reduced to $<10^{-9}$ Torr while maintaining a constant substrate temperature of 760°C. A number of important features are observed after opening the Ga shutter. The initially low Ga desorption flux seen in Figure 2 indicates that Ga adsorbs in a strongly bound site that is characterized by a long residence time. We also see in Figure 2 that H_2 is a byproduct of this adsorption process. After deposition of roughly one monolayer, the Ga desorption increases and the H_2 desorption decreases, indicating the presence of a second, weakly bound state. These results are consistent with the findings of Jones et. al [3] and Lee et. al [5] who both proposed that Ga exists in two adsorption sites during growth. After this initial Ga pulse, we close the Ga shutter and allow the excess Ga to desorb from the surface. Subsequent exposure to incident Ga results in only the higher Ga desorption flux, with no detectable change in the H_2 desorption, and no reduced desorption flux indicative of the strongly bound Ga. We can again prepare a surface that will adsorb Ga in the strongly bound sites by exposing the surface to NH_3. The procedure outlined above can be used to detect the presence of these sites.

Measurement of the RHEED intensity as shown in Figure 2 and Figure 3 reveals that two slope maxima occur during the initial transient RHEED decrease. Quantitative information can be extracted from this RHEED intensity variation by definition of the time interval, Δt, as shown in Figure 3. We find that the time dependence of the transient Ga and H_2 desorption track this RHEED intensity variation as indicated in Figure 2. Based on this observation we believe that Δt gives an estimate of the time required for saturation of the strongly bound Ga sites. The quantity 1/Δt decreases linearly with increasing NH_3 beam equivalent pressure (BEP), while it increases linearly with incident Ga flux. Furthermore, this behavior is observed only when the incident Ga exceeds the available N provided by the incident NH_3.

Based on these transient data, we have identified two Ga adsorption sites. We will present evidence in the next section that the more tightly bound Ga site contributes to growth, whereas the weakly bound Ga acts to inhibit growth by blocking the strongly bound Ga, and inhibiting the incorporation of N from NH_3.

3.2. Steady State Growth Behavior

RHEED indicates that high Ga flux and high substrate temperature are necessary to achieve atomically smooth surface morphology. The objective of this section is to examine the growth kinetics when the incident Ga exceeds the available N provided by NH_3.

In Figure 4 and Figure 5 we see the desorbed H_2, N_2, and Ga fluxes resulting from exposure of the GaN surface to a 15 second pulse of Ga while the NH_3 BEP is held constant. Changes in other detected species such as NH_x complexes or atomic N were too small to measure. For the data shown in Figure 4 the Ga flux was 4.2×10^{14} cm^{-2}s^{-1} whereas in Figure 5 it was increased to 1.4×10^{15} cm^{-2}s^{-1}. All other growth parameters were the same for both plots. The increased H_2 desorption during growth is attributed to the forward reaction

$$2\,Ga + 2\,NH_3 \rightarrow 2\,GaN + 3\,H_2$$

(1)
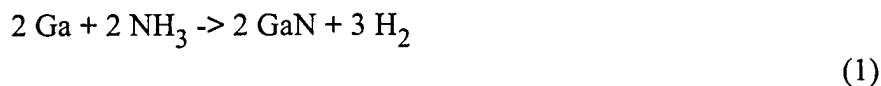
In the absence of incident Ga we find that contributions from the reaction

$$2\,NH_3 \rightarrow N_2 + 3\,H_2$$

(2)

become significant at substrate temperatures exceeding 800°C, and we have not yet determined the relative contributions of the two reactions during and prior to growth at elevated temperatures. At temperatures below 800°C, however, we believe that ΔH_2 yields a reliable estimate of the growth rate. The accuracy of this technique is currently being investigated using post growth film thickness measurements. In Figure 5 we see that initiation of growth causes a transient pulse of H_2 to desorb from the surface, whereas in Figure 4 the desorbed H_2 flux reaches its maximum value at steady-state. In general, we find that the desorbed H_2 flux during steady-state growth increases linearly with increasing Ga flux, but then decreases as the Ga flux exceeds a saturation value. This relationship is shown in Figure 6, where we see the dependence of ΔH_2 on the incident Ga flux at three different substrate temperatures.

In Figure 6 we see that high Ga flux causes a reduction in the growth rate, but that increasing the substrate temperature minimizes this effect. A temperature gradient of about 30°C exists across the substrate [6] which introduces unertainty to the data shown in Figure 6. This uncertainty arises from the fact that DMS measurements integrate the desorbed flux over the whole sample. This effect is particularly pronounced at high incident Ga flux, where the growth rate is strongly temperature dependent. This temperature gradient also makes verification of the DMS data difficult, since film thickness measurments are dependent on the location on the sample where the film thickness is measrued. These difficulties can be overcome by conducting the same measurments on samples that are known to be isothermal, and work is currently underway to achieve this goal.

In spite of the problems introduced by the temperature gradient, we are confident that the data in Figure 6 yield an accurate picture of the general relationship between growth rate, fluxes, and substrate

temperature. The reduced growth rate at high Ga flux can be accounted for by consideration of the following simple kinetic model. We start by making a number of assumptions about the atomistic behavior of adsorbed Ga which will be justified by agreement with measured data. First, based on the DMS measurements presented in section 3.1 we consider Ga in the weakly bound state. The fractional area of the surface covered by weakly bound Ga is σ_{Ga}. The second assumption is that Ga desorption occurs only from this weakly bound state, which results in a Ga desorption term that is proportional to σ_{Ga}. We assume that for complete coverage ($\sigma_{Ga} = 1$), the desorption flux is equal to the evaporation rate of Ga from liquid Ga as developed in ref. [6] , and therefore we approximate the Ga desorption rate as $\sigma_{Ga}F_0(T_{sub})$, where $F_0(T_{sub})$ is the desorption flux of Ga vapor leaving liquid Ga. This assumption is consistent with the temperature dependence of the Ga desorption data as measured using DMS. This model does not require that Ga completely wet the GaN surface, since the shadowing effect of droplets could account for the observed behavior as well. In the limit of complete wetting, σ_{Ga} is the Ga surface coverage. Direct measurement of σ_{Ga} is complicated by the temperature gradient discussed earlier [6] , and we have been unable to obtain a reliable measure of σ_{Ga} due to the strong temperature dependence of the coverage.

The DMS measurements shown in Figure 6 indicate that excess Ga reduces the growth rate. We assume that NH_3 reacts only with the strongly bound Ga, and that the excess Ga in the weakly bound sites reduces the growth rate by blocking the underlying reactive Ga sites. Further motivation for such a growth mechanism can be found in the work of Liu and Stevenson [7] , who found that the coexistence of Ga and GaN enhanced the decomposition of NH_3 relative to Ga alone.

We let the growth rate be proportional to the fraction of strongly bound Ga sites that are exposed to the incident NH_3, ($1-\sigma_{Ga}$). We now consider the following quantities:

F_N= total available incident N flux provided by the NH_3

F_{Ga}= total available Ga flux

$\sigma_{Ga}F_0(T_{sub})$= Ga desorption flux where all temperature dependence will be included in the Ga desorption term, $\sigma_{Ga}F_0(T_{sub})$. DMS measurements of both the H_2 and Ga desorption fluxes show that the NH_3 reactivity does not depend on substrate temperature over the range (700°C-820°C), and we therefore let F_N be independent of substrate temperature. We wish to determine the steady-state growth rate when $F_{Ga}>F_N$. The time derivative of the Ga coverage is given by

$$\frac{1}{A}\frac{dN_{Ga}}{dt} = F_{Ga} - F_N(1-\sigma_{Ga}) - \sigma_{Ga}F_0(T_{sub})$$

(3)

where the growth rate is $F_N(1-\sigma_{Ga})$, and N_{Ga} is the number of free Ga atoms on the surface. The substrate surface area is A. Solving equation 3 for σ_{Ga} at steady-state gives the growth rate

$$F_N(1-\sigma_{Ga}) = F_N\left(\frac{F_{Ga}-F_N}{F_0(T_{sub})-F_N}\right)$$

(4)

The results of this model are shown as solid lines in Figure 6. As stated earlier, we estimate the desorption term $F_0(T_{sub})$ from the equilibrium vapor pressure of Ga over liquid Ga given in ref. [8] . We

see from <u>Figure 6</u> that the measured data is in reasonable agreement with the steady-state solution given in <u>equation 4</u>. The only parameter used to fit the predictions of <u>equation 4</u> to the measured data was F_N, which is equated to the known Ga flux for which ΔH_2 is maximum. The main points to be extracted from this discussion are that excess Ga reduces the formation rate of GaN, and that this effect can be minimized by increasing the substrate temperature. Additionally, we see that a drastic reduction in growth rate occurs when $F_{Ga}=F_0(T_{sub})$, where $\sigma_{Ga}=1$ and growth is inhibited. We can also explain the increase in H_2 desorption observed after closing the Ga shutter as seen in <u>Figure 5</u> as follows. During growth, excess Ga resides on the surface and reduces the growth rate by blocking the reactive sites. After closing the Ga shutter, the excess Ga is depleted either by evaporation or by reaction with the GaN surface. As more surface area is exposed, the growth rate increases for a short time while the remaining surface Ga reacts with NH_3 on the exposed GaN surface, resulting in the short pulse of H_2 desorption from the surface.

3.3. Conclusions

Analysis of the transient H_2 and Ga desorption, along with the specular RHEED intensity show that Ga resides on the surface in both weakly bound and a strongly bound sites. After saturation of the strongly bound Ga sites, the Ga desorption flux increases, indicating the presence of the more weakly bound Ga. The adsorption process of Ga into the strongly bound sites produces H_2 as a byproduct.

Analysis of the steady-state growth rate using DMS shows that excess Ga reduces the growth rate. A rate equation giving the steady-state value of the Ga coverage in the weakly bound state was described. The key feature of this model is the blocking of reactive sites by the weakly bound Ga. The model shows that by increasing the substrate temperature, the growth rate can be increased due to reduced coverage of this excess Ga.

Acknowledgments

References

[1] S. Strite, H. Morkoç, *J. Vac. Sci. Tech. B 10*, 1237-1266 (1992).

[2] N.-E. Lee, R.C. Powell, Y.-W. Kim, J.E. Greene, *Journal of Vacuum Science and Technology A 13*, 2293 (1995).

[3] C.R. Jones, T. Lei, R. Kaspi, K.R. Evans, unpublished (1995) 0.

[4] N Newman, J Ross, M Rubin, *Appl. Phys. Lett. 62*, 1242-1244 (1993).

[5] R. C. Powell, N. -E. Lee, W. -W. Kim, J. E. Greene, *J. Appl. Phys. 73*, 189-204 (1993).

[6] R. Held, D. Crawford, A. M. Johnston, A. M. Dabiran, and P. I. Cohen, submitted to J. Electr. Mat. (No journal name recognized.)

[7] S. S. Liu, D. A. Stevenson, *J. Electrochem.Soc. 125*, 1161 (1978).

[8]CRC Handbook of Chemistry and Physics, 72nd Edition. p. 5-69 Editor: D. R. Lide (1991-1992) (No journal name recognized.)
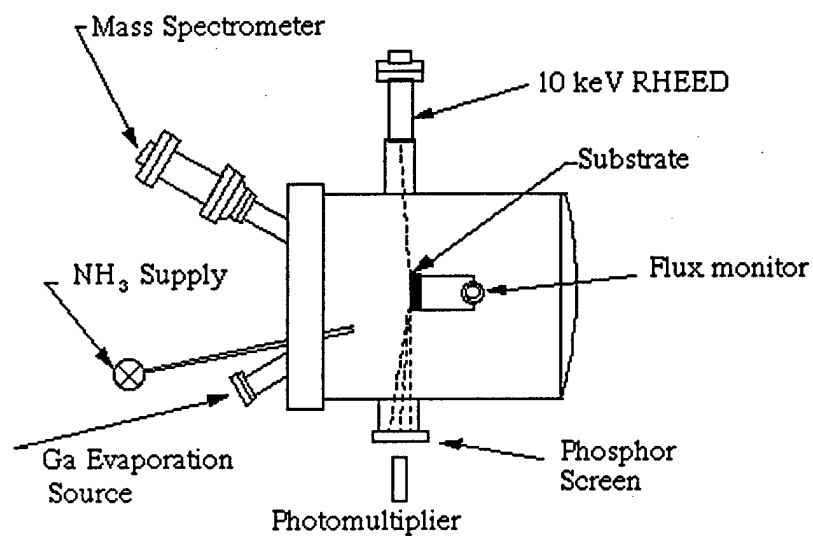
Figures

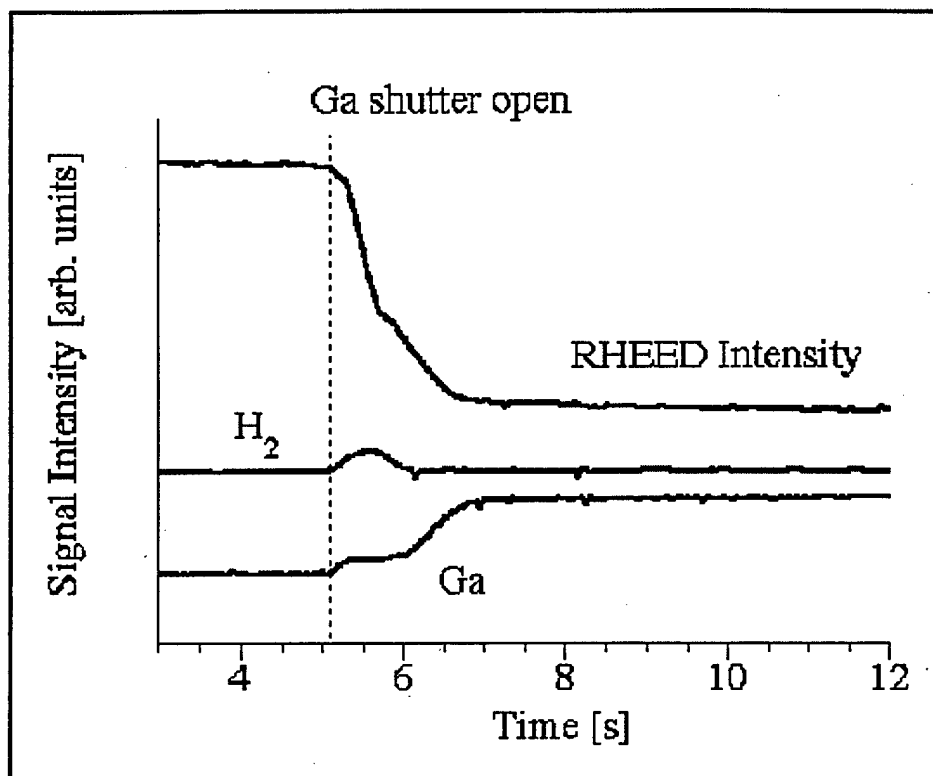**Figure 1.** Schematic diagram of the Gen II MBE system used for growth.

Figure 2. The transient response of the Ga and H_2 desorption to a step-function of incident Ga is shown in the absence of incident NH_3. The response of the specular RHEED intensity observed along the <011$\bar{2}$> azimuth is also shown. (F_{Ga}=1.6x10^{15} cm^{-2}s^{-1}, T_{sub}=760°C).
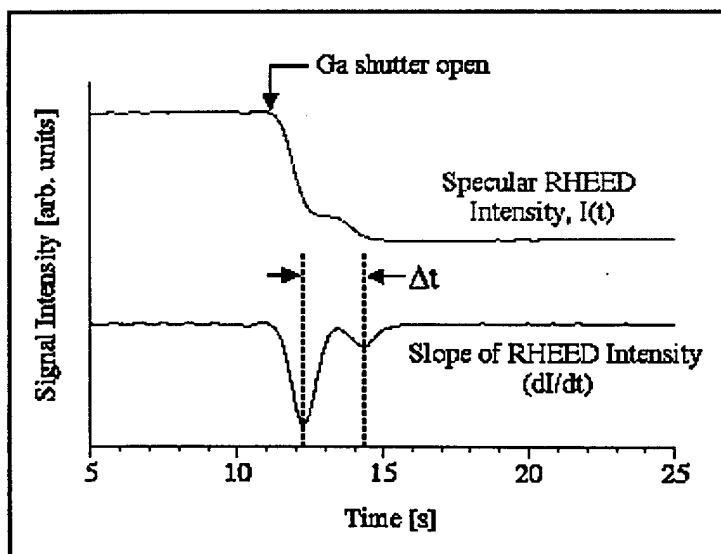

Figure 3. Specular RHEED intensity and its first derivative. Differentiation of the signal allows quantitative analysis of the transient signal. Experimental conditions for the data shown here are T_{sub}=780°C, NH_3 BEP=1.1x10^{-5} Torr. F_{Ga} = 1.45ML/s.
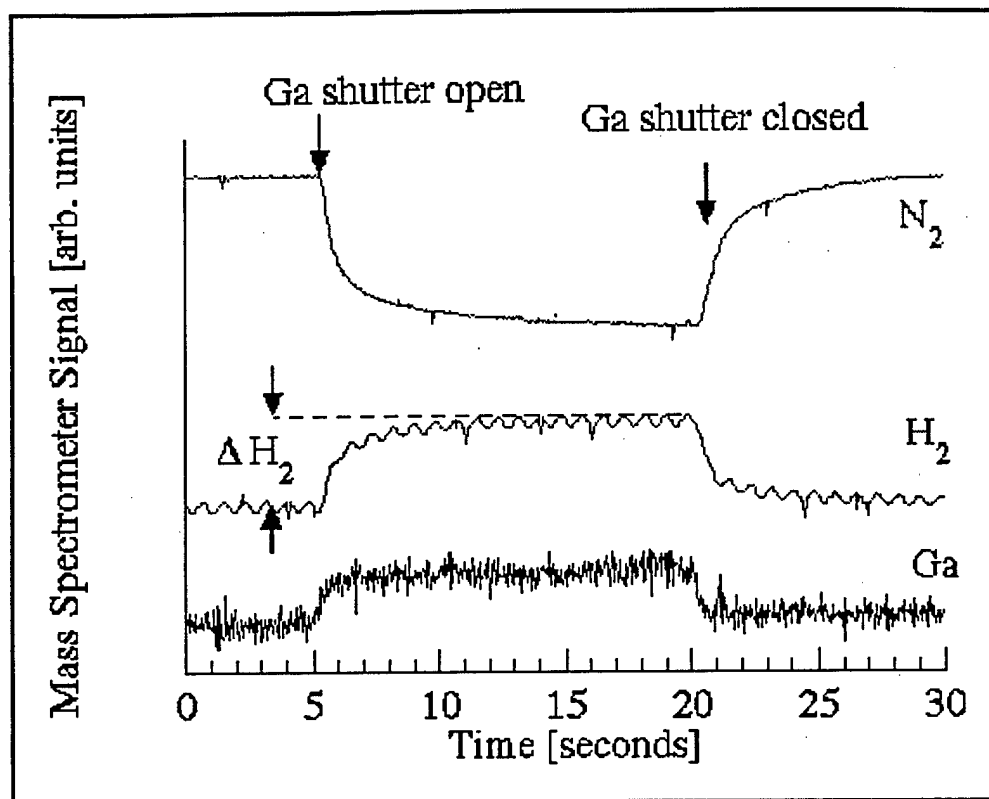
Figure 4. Changes in the N_2, H_2 and Ga desorption are caused by exposing a smooth GaN sample to a 15 second pulse of incident Ga under N rich growth conditions. Substrate temperature=820°C, NH_3 beam equivalent pressure = 7×10^{-6} Torr, Ga flux =4.2×10^{14} cm^{-2}s^{-1}. The high frequency H_2 signal oscillations arise from fluctuations in H_2 background pressure caused by temperature cycling of the cryopumps.
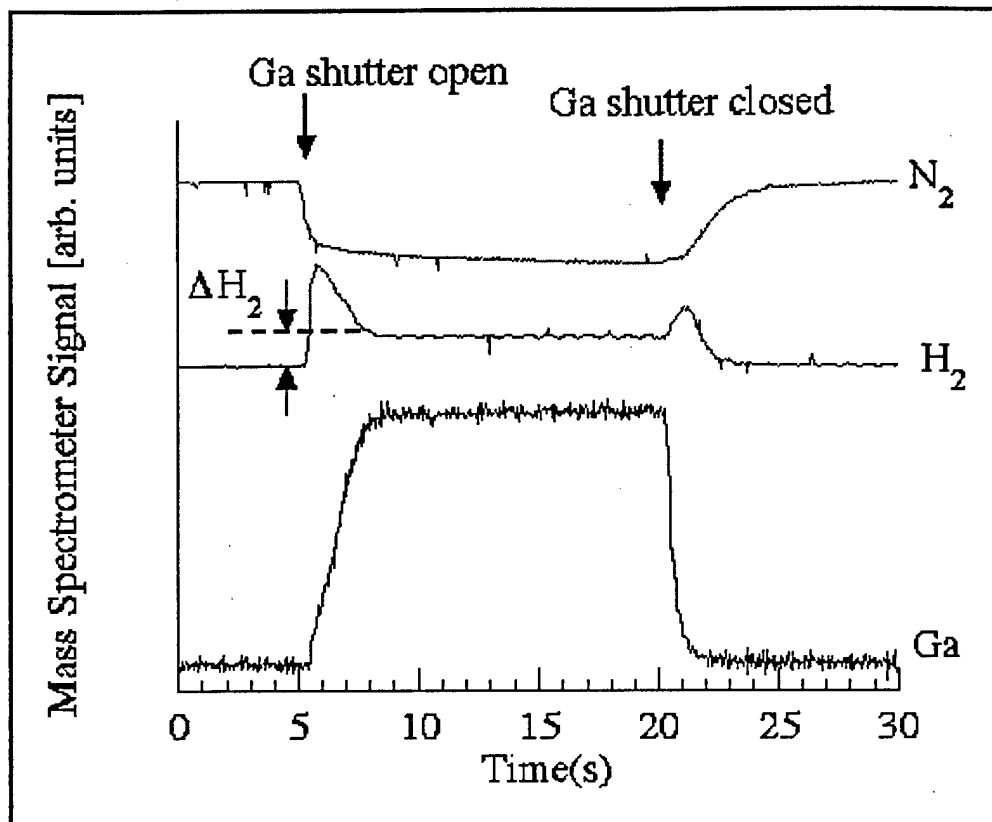
Figure 5. Changes in the N_2, H_2 and Ga desorption are caused by exposing a smooth GaN sample to a 15 second pulse of incident Ga under Ga rich growth conditions. Substrate temperature=820°C, NH_3 beam equivalent pressure = 7×10^{-6} Torr, Ga flux =1.4×10^{15} cm^{-2}s^{-1}. The H_2 signal oscillations arise from fluctuations in H2 background pressure caused by temperature cycling of the cryopumps.
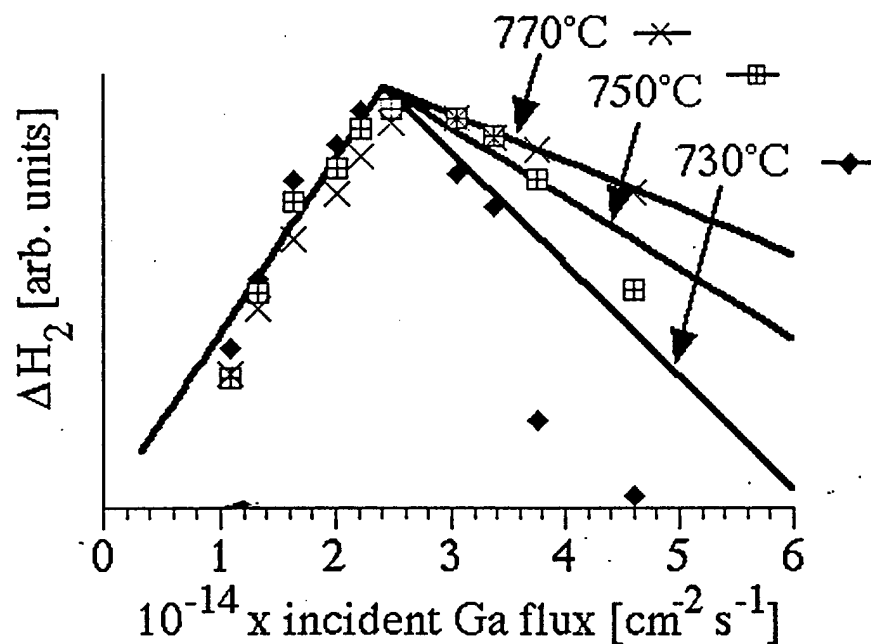
Figure 6. Dependence of ΔH_2 on the incident Ga flux. The lines show the theoretical incorporation rate based on the simple kinetic model presented in this paper.

© 1996 The Materials Research Society

MRS Internet Journal Nitride Semiconductor Research

2.4

In Situ Control of GaN Growth by Molecular Beam Epitaxy

R. HELD,* D.E. CRAWFORD, A.M. JOHNSTON, A.M. DABIRAN, and
P.I. COHEN*

Department of Electrical Engineering, University of Minnesota, Minneapolis,
MN 55455

Methods to determine GaN surface temperature, surface composition, and growth rates using *in situ* desorption mass spectroscopy (DMS) and reflection high energy electron diffraction (RHEED) are demonstrated for molecular beam epitaxial growth of GaN using NH_3. Using these methods, the GaN surface temperature, T_s, and GaN growth rates as a function of T_s, Ga flux, and NH_3 flux were obtained. Surface temperatures were determined from DMS and RHEED measurements of the temperature at which Ga condenses on GaN. NH_3-limited and Ga-limited growth regimes are identified and the transition between these regimes is shown to be abrupt. NH_3-limited samples have a weakly reconstructed (2×2) RHEED pattern, while Ga-limited samples reveal a transmission pattern. Atomic force microscopy showed that NH_3-limited samples exhibit atomic steps while Ga-limited samples exhibit faceting.

Key words: Atomic force microscopy (AFM), GaN, molecular beam epitaxy (MBE), reflection high energy electron diffraction (RHEED)

INTRODUCTION

GaN is a direct, wide bandgap semiconductor making it attractive for blue light emitting diodes (LEDs) and lasers. Further, it is suitable for use in high temperature applications and corrosive environments. Since the mid 80s, major efforts have been underway to produce high quality material using a variety of growth methods as reviewed by Strite and coworkers.[1] The growth has proven difficult. Among the multiple problems in growing high quality material by molecular beam epitaxy (MBE), which is the focus of this discussion, is the accurate determination of growth conditions, including surface temperature, growth rates, and surface composition. The purpose here is to examine the use of *in situ* reflection high energy electron diffraction (RHEED) and desorption mass spectroscopy (DMS) for atomic level control of GaN growth.

*Also, Department of Chemical Engineering and Materials Science, University of Minnesota, Minneapolis, MN 55455
(Received September 24, 1996; accepted December 2, 1996)

The surface temperature of a sample in MBE growth is usually determined by using a thermocouple, infrared (IR) pyrometry, surface reconstruction transitions,[2] the oxide desorption temperature, or the temperature dependence of the optical band edge.[3] However, none of these techniques are adept at accurately determining surface temperature in a typical MBE environment suitable for III-N materials, where sample mounting is problematic and temperatures of up to 1000°C are typical. In particular, GaN does not have a congruent sublimation temperature or a well-defined oxide desorption temperature. Therefore, simple methods comparable to the GaAs system are not applicable. To address this problem, we have developed a novel *in situ* method to determine GaN surface temperatures using either DMS or RHEED.

To accurately set growth conditions, it is important to know the growth rate as a function of surface temperature and fluxes. So far, most existing growth rate data on GaN were obtained by *ex situ* thickness measurements, which even when a superlattice is grown require long growth times for each data point. Some *in situ* methods were reported, for example, using the period of RHEED intensity oscillations[4,5]
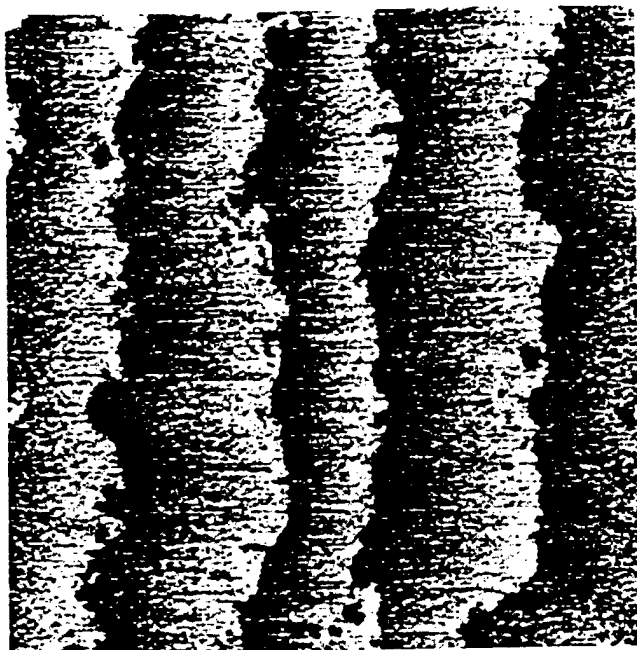
18

Fig. 1. A 500 × 500 nm AFM image of an atomically smooth Al_2O_3 substrate after being cleaned in acetone and methanol, followed by an etch in 1:1 H_3PO_4:H_2SO_4. Each step was performed at 65°C for 5 min, followed by a final deionized water rinse and rapid drying with high purity N_2. The steps are about 1000Å in width.

and IR interference,[6] but little growth rate data is published. We will present incorporation data obtained using *in situ* real-time DMS and identify different growth regimes for MBE growth of GaN using NH_3.

The next section contains general information about sample preparation and the experimental setup. In the Results and Discussion section, DMS and RHEED measurements are presented that describe the main adsorption behavior of Ga on GaN. Also in this section is a discussion combining RHEED and DMS to determine the surface composition of GaN and its control. Based on those observations, techniques are developed in a section entitled Surface Temperature Determination to measure GaN surface temperatures. The measurement of growth rate is then described. In the last subsection, the surface morphology obtained under different growth conditions is discussed. The results are summarized in the last section.

EXPERIMENTAL

For our DMS and RHEED measurements we used one inch, polished c-plane Al_2O_3 substrates. The substrates were cleaned for 5 min in acetone and methanol, followed by a 5 min etch in 1:1 H_3PO_4:H_2SO_4. Each step was performed at 65°C, followed by a final deionized water rinse and rapid drying with high purity N_2. Atomic force microscopy (AFM), as shown in Fig. 1, confirmed atomically smooth substrates featuring atomic steps of about 1000Å in width. A 2000Å Ti coating was applied to the back of the substrates by e-beam evaporation in a separate chamber. The coating serves to increase the heat absorbed by radiation and

to assist even heat distribution.

Mounting arrangements involving In bonding were found to be unreliable due to evaporation at the high substrate temperatures used in AlN and GaN growth, resulting in hot spots and eventual loss of the sample. Clips that applied even slight pressure induced unwanted stress onto the sample and caused sapphire to crack during thermal cycling. Instead we used a mount which holds the sample loosely without stress. The coated sapphire substrate was heated directly by radiation from a resistive heater. A thermocouple touched the back of the heater, introducing an offset between the sample surface and thermocouple reading. This offset varied between 50 to 150°, depending upon the growth temperature, as well as from run to run, depending on the details of the sample mounting arrangement.

Prior to growth, the substrates were outgassed for several hours at 300°C in the preparation chamber of the MBE system, followed by 1 h at 500°C in the growth chamber. The NH_3 leak valve was set to produce a beam equivalent pressure (BEP) of 1×10^{-5} Torr, as determined by a Bayard-Alpert ionization gauge which remained positioned close to the sample location during the measurement. Then the substrate temperature was ramped at 100°/min from 500 to 1000°C for a 15 min surface nitridation. AFM showed that the surface remained atomically smooth after this Al_2O_3 nitridation. A 250Å AlN buffer layer was then grown at 1000°C using an Al flux of 1.2×10^{14} cm^{-2} s^{-1} (equivalent to 0.10 ML/s AlN) as determined by AlAs RHEED intensity oscillations. RHEED showed a transmission pattern during and after AlN growth. The Ga shutter was then opened to provide a flux of 1.1×10^{15} cm^{-2} s^{-1} (or 1.0 ML/s GaN) and the sample temperature was ramped down at 100°/min to 800°C. The Al shutter was closed during the ramp below about 900°C. Finally, a 2500Å GaN buffer layer was grown at 800°C. RHEED showed a weakly reconstructed (2×2) pattern after the GaN buffer layer was completed.

A 10 keV electron gun was employed for RHEED measurements of the specular intensity without energy filtering. Measurements were made with the electron beam directed along the GaN $\langle 1\bar{2}\bar{2}0 \rangle$ azimuth. The diffracted intensity of the specular beam was measured using a phosphor screen and a photomultiplier tube.

Our DMS apparatus is based on a differentially pumped UTI 100C quadrupole mass-spectrometer mounted on one of the source flanges of the MBE system. A similar apparatus has been used by Tsao et al.[7] to study GaAs growth kinetics, and by Jones et al.[8] for GaN growth. The solid angle seen by the DMS is limited by the cryoshroud in the growth chamber to subtend only the region around the sample holder. For a few of the measurements to be presented, additional collimation was added in order to limit this region so that only the center of the sample contributed to the desorption signal. This additional collimation reduced the effect of a temperature gradient as

well as the background contribution of surrounding cooler surfaces. Since only a small portion of the sample was subtended, the collimation also reduced the signal-to-noise ratio. Those measurements performed with the additional collimation are indicated.

RESULTS AND DISCUSSION

The growth kinetics of GaN by MBE using NH_3 are complicated by the temperature dependence of the dissociation and incorporation of NH_3, and the temperature and compositional dependence of the residence times of the reactants on the GaN surface. This means that without knowledge of the microscopic surface processes it is not clear how to set optimum growth parameters. Since the flux and temperature dependencies of the Ga and N surface coverages are not well known, the species that limit the growth cannot be easily identified. To monitor these growth processes, structural and compositional changes at the surface can be measured with RHEED; changes in the species leaving the surface can be measured with DMS. These two techniques complement each other in determining microscopic processes.

The main point of the measurements to be presented can be understood by considering the adsorption of Ga onto an otherwise inert surface in the absence of NH_3. Examine two limits: First, at sufficiently high temperature, an incident Ga flux will produce a steady state Ga coverage that depends on the incident Ga flux and the Ga residence time. In this steady state, the total amount of adsorbed Ga is constant so that the incident flux must equal the desorbing flux. Second, if the substrate temperature is decreased sufficiently, there will be a temperature below which Ga condenses on the surface forming multilayers and/or droplets. Below this temperature, the system is not in steady state since the incident flux exceeds the desorbing flux, and Ga is adsorbed continuously. The transition from steady state to condensation is sharp and can be determined by measuring the temperature at which the desorbed Ga flux begins to decrease. For a given incident Ga flux, this transition corresponds to a unique surface temperature well described by equilibrium vapor pressure data.

Employing DMS and RHEED, the adsorption behavior of Ga on Ga terminated GaN will be shown to follow this model over a significant range of temperatures. Over this range, the decomposition of GaN can be neglected compared to the incident and desorbing fluxes. Further, above the condensation temperature, the difference between the desorbed flux with and without NH_3 can be used to measure growth rate. Using RHEED and DMS, we will identify the conditions for Ga condensation and present methods to determine surface composition. Employed together, these techniques can be used to set growth conditions.

Ga Condensation

The key adsorption behavior can be seen in the RHEED data of Fig. 2, which shows the specular

RHEED intensity from a GaN surface during and after Ga exposure at three different substrate temperatures. From this data, taken at a high Ga to NH_3 ratio, one can identify the surface temperature for Ga condensation. The Ga shutter is opened at time t_1 and then closed at t_4. The incident Ga and NH_3 fluxes were the same for all three curves. The starting RHEED intensity depends only on sufficient initial NH_3 exposure in the absence of Ga, as covered later, and is relatively independent of typical growth temperatures and absolute NH_3 flux. Three distinct behaviors are observed: Curve (a), measured at $T_s = 800°C$, shows, between t_1 and t_3, an initial rapid decrease to a value that is relatively constant, and then at time t_4 a rapid recovery. Curve (b), measured at a temperature 5°C lower, shows a similar but larger decrease to a constant value, as well as a similar rapid recovery. And curve (c), reduced by an additional 5°C, shows a similar initial behavior but then a steady decrease, followed by a two stage recovery having a slow and fast component. We will interpret the transition between curve (b) and (c) to correspond to the temperature, T_c, at which Ga condenses. This transition is very abrupt—a temperature change of a few degrees is sufficient for its observation. The interpretation of the two-step recovery requires a model for the formation of GaN at the surface. At this point, we note that the fast recovery only occurs if there is an NH_3 flux present. This is a robust measurement, essentially independent of scattering angle.

Note that the features illustrated in Fig. 2 are only observed under an excess of Ga. By contrast. under excess NH_3 on a sufficiently smooth surface, the
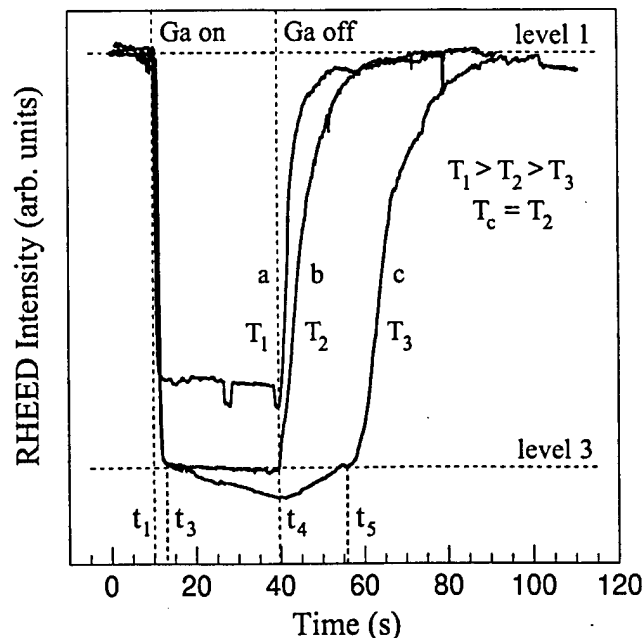

Fig. 2. Intensity variation of the specular RHEED beam along the $\langle 1\bar{2}20 \rangle$ azimuth during opening and closing of the Ga shutter in an NH_3 flux for (a) above, (b) at, and (c) below the condensation temperature. Curve (a) corresponds to a partial layer of weakly adsorbed Ga and partial nitridation, curve (b) to a complete layer of weakly adsorbed Ga, and curve (c) to Ga condensation.
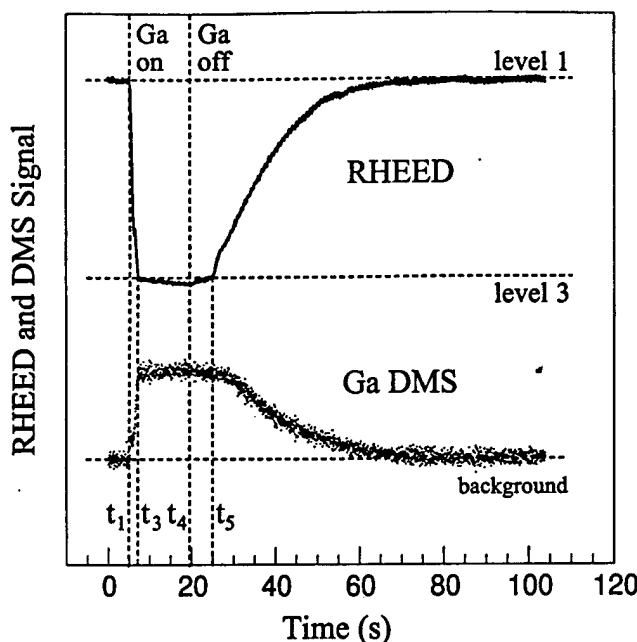
Fig. 3. RHEED and uncollimated Ga DMS signal during Ga accumulation below the condensation temperature. After the Ga shutter is closed at t_4, Ga desorption remains constant until part of the GaN surface is exposed at t_5. At the same time, the RHEED intensity increases slowly up to t_5 where a large change in slope takes place. The slow decrease of the DMS signal after t_5 is due to the temperature gradient across the sample, resulting in unsynchronized completion of Ga desorption from the surface.
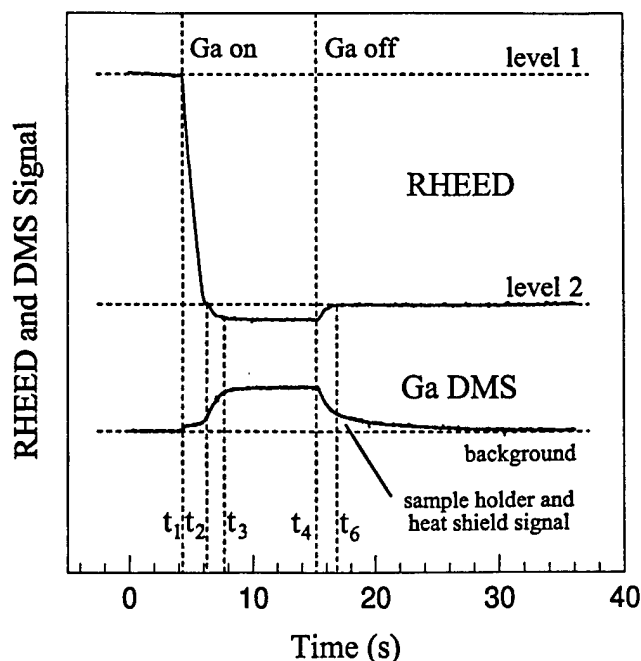

Fig. 4. RHEED and uncollimated Ga DMS signal without NH_3 flux above the condensation temperature. Level 1 indicates a nitrided starting surface, while a stable level 2 is reached after Ga exposure, indicating a Ga terminated surface. Note that during Ga exposure, the intensity level reaches steady state below level 2 suggesting fractional Ga coverage.

diffracted intensity can show damped intensity oscillations,[5,4,13] rather than the behavior of Fig. 2. Continued growth under those conditions, however, eventually leads to a transmission RHEED pattern.

Since similar decreases in the diffracted intensity could result from changes in surface composition, structure, and morphology, it is important to correlate these measurements with other probes. Figure 3 compares a DMS measurement of the desorbed Ga vs time to the corresponding RHEED measurement made at a temperature below T_c, where Ga condenses on the surface. To improve the signal-to-noise ratio, we did not collimate the mass spectrometer for this set of measurements and therefore an average over the entire surface of the one inch sample is obtained. The RHEED measurement, on the other hand, is more localized; and by moving the beam across the surface, we determined that there was an approximately 30° temperature gradient across the sample surface. After opening the Ga shutter at t_1, the decrease in the RHEED intensity parallels an increase in the Ga DMS signal to a steady state value at t_3. There is a slight decrease in the RHEED intensity after t_3 due to increased attenuation of the signal originating from ordered regions. By contrast, the Ga DMS signal is constant after t_3. This is consistent if the desorption energies from successive layers are approximately equal. The magnitude of this desorbed Ga is independent of temperature above T_c and below T_c it decreases due to condensation. Below T_c, this desorption flux is approximately equal to the flux from liquid

Ga following the temperature dependence of the equilibrium vapor. The recovery behaviors of the two signals after the Ga source is shuttered are also correlated to an extent—the DMS indicates that the increase in the diffracted intensity can be associated with a decrease in the amount of adsorbed Ga and not just to a coalescence of surface adatoms that reduces the step density. The correlation is not exact, however. After the Ga source is shuttered at t_4, the RHEED intensity increases slightly until, at t_5, there is a rapid increase. By contrast, the DMS signal remains constant during this time and then decreases to a background. This difference in recovery rates would be expected if regions on the sample surface at lower temperature, where there is a larger amount of condensed Ga to desorb, also contribute to the DMS signal. Thus, the condensation is seen in both the RHEED and DMS data, though the regions sampled can be quite different, as discussed later.

Surface Composition

The composition of the GaN surface can be manipulated by reaction with NH_3 or Ga, and both DMS and RHEED can be used as a monitor. These surfaces have been determined to have a GaN(0001)A orientation.[9,10,12] Exposure to an NH_3 flux for a long time will cause it to be nitrided. As illustrated in Fig. 2, this procedure brings the RHEED intensity to level 1. This is a stable surface even if the NH_3 flux is removed and serves as the starting surface for the measurements in Fig. 4.

Figure 4 then compares RHEED and DMS mea-

surements for a surface with no NH_3 flux. For these data, collimation was not used. A substrate temperature above that for Ga condensation was chosen. The Ga shutter was opened at t_1 and the RHEED intensity decreased to a steady state value at t_3, after going through a change in slope at t_2. The time to reach this steady state depended on the Ga flux. Since this is a steady state condition, the Ga desorption flux is equal to the incident flux. Further, since there is no NH_3 flux, when this steady state is reached, the incident Ga will have had time to react with all of the active nitrogen on the surface. The Ga shutter was then closed at t_4, at which time the RHEED intensity increased until it reached at t_6 an intensity marked level 2, and the DMS signal simultaneously decreases to a background. Since the final RHEED intensity was independent of the steady state Ga coverage that was achieved during deposition where the RHEED intensity was below level 2, we interpret this remaining layer to be strongly bound Ga that would make up the bulk termination layer of GaN(0001)A. It does not leave the surface as easily as the excess Ga, i.e., Ga weakly bound to Ga terminated GaN. At typical growth temperatures, this Ga terminated surface is stable in the absence of either Ga or NH_3.

If the surface is subsequently reacted with NH_3, the behavior seen in Fig. 2 is obtained and the RHEED intensity rises to the nitrided value of level 1. These observations indicate that there are at least two stable surface terminations possible on GaN(0001)A— one is reached after a GaN surface is exposed to an NH_3 flux in the absence of Ga (level 1), and the other is obtained after Ga exposure, followed by an anneal in the absence of both NH_3 and Ga (level 2).

These two surfaces could subsequently be reacted with NH_3 or Ga. Reacting the nitrided surface with Ga gives rise to a hydrogen peak in the DMS, indicating that this surface contains H.[11,12] In the case of Ga-termination, the surface can be exposed to a N-supplying flux to examine the reactivity of nitrogen bearing species.[13]

The picture that emerges is illustrated in Fig. 5 where weakly bound Ga is shown adsorbed on Ga terminated GaN. In this situation, if there were no NH_3 or Ga flux present, the excess Ga desorbs, leaving a Ga terminated GaN surface. If now an NH_3 flux is provided, the Ga termination layer would react giving a nitrided surface. If then a Ga flux is provided to this nitrided surface, in the absence of NH_3, the Ga would react forming GaN and causing hydrogen to desorb. After the nitrogen is consumed, a surface coverage of Ga will build up. If the substrate temperature is above the condensation temperature only a weakly bound Ga layer, likely less than a monolayer, is in steady state, as shown in Fig. 5a. If the substrate temperature is below the condensation temperature for that Ga flux, Ga multilayers and/or droplets will form, as shown in Fig. 5c. The crossover between steady state Ga coverage and condensation is shown in Fig. 5b. Once the Ga flux is stopped, any weakly bound Ga will again desorb to eventually expose the Ga termination layer.

Surface Temperature Determination

The implications of the observations described so far are that the Ga condensation temperature on Ga-terminated GaN is a function of the incident Ga flux and that this condensation temperature is determined by the detailed balance of the incident Ga flux and the flux evaporating from liquid Ga. Therefore, to calibrate the substrate thermocouple, we only need to know this incident flux, which can be measured using GaAs RHEED intensity oscillations. Using either RHEED or DMS observations, at a given incident Ga flux, we find the lowest temperature at which the incident flux equals the desorbing flux, i.e., the onset of Ga condensation. We then determine the temperature offset of the thermocouple reading by setting the known incident flux equal to the flux corresponding to the equilibrium vapor as follows:

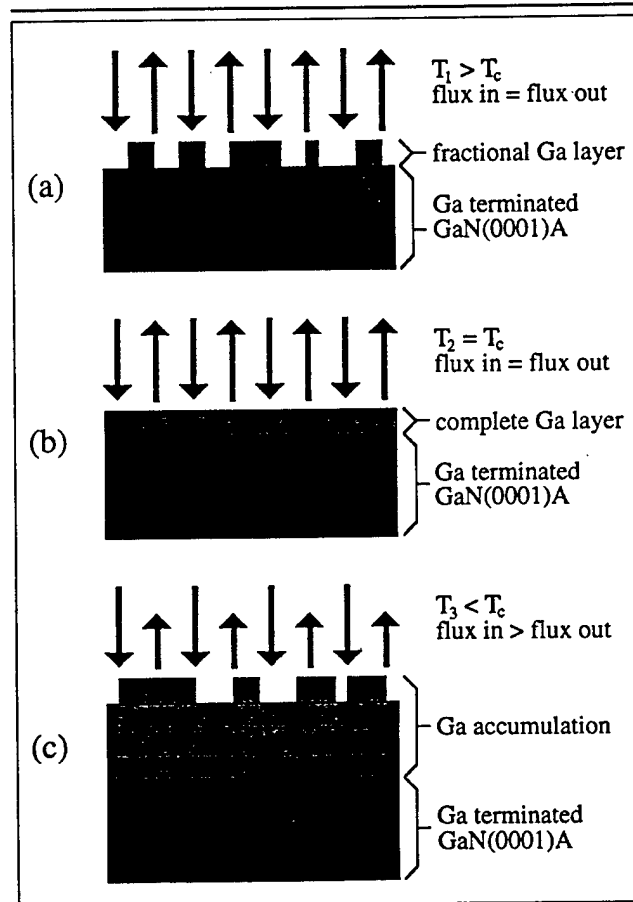$$\Gamma_{in} = \frac{p_{eq}}{\sqrt{2\pi mkT_c}} \qquad (3.1)$$

Fig. 5. Behavior of incident Ga on a rigidly attached (strongly bound) Ga termination layer as a function of temperature. Above the condensation temperature (a) steady state partial Ga coverage is obtained, and the incident flux equals the desorbing flux. Complete steady state Ga coverage is obtained at a critical temperature, (b) below which Ga condensation takes place. Note that the incident flux still equals the desorbing flux. Below this critical temperature (c), Ga multilayer accumulation takes place and the incident flux exceeds the desorbing flux.
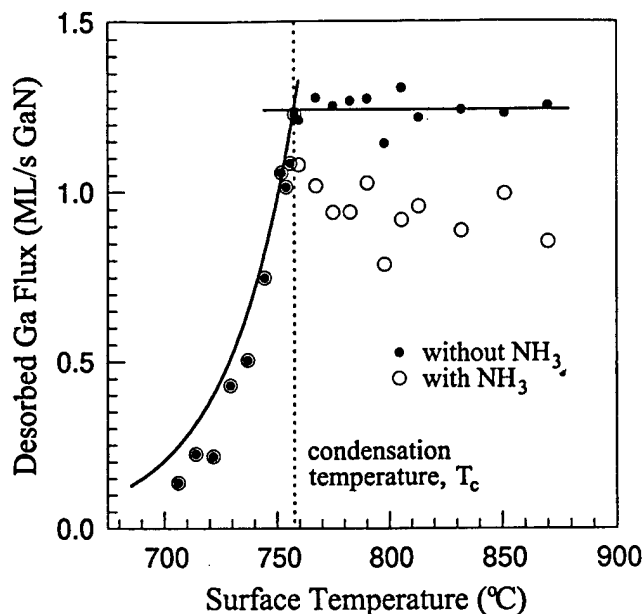
Fig. 6. Condensation temperature determination using collimated Ga DMS with and without NH_3 for an incident Ga flux of 1.25 ML/s GaN. Without NH_3 the DMS signal remains constant above the condensation temperature, while with NH_3 the signal is reduced due to GaN formation. The condensation temperature is found as illustrated by observing the temperature at which the signal drops exponentially without NH_3 or by observing the change of slope and subsequent exponential drop with NH_3. The solid curve at temperatures below T_c is calculated from Ga vapor pressure data. (The data presented in this figure should not be used for growth rate determination since steady state was not obtained.)

where p_{eq} is usually tabulated as:[14]

$$\log(p_{eq}) = A + BT^{-1} + C \log T \qquad (3.2)$$

with p given in units of atm., A = 6.754, B = −13984, and C = −0.3413. Here Γ_{in} is the incident Ga flux and $T = T_c$.

Alternatively, both the incident and desorbing fluxes can be expressed more symmetrically by measuring the incident flux in GaN monolayers per second, $1/\tau_i$, and by fitting the flux desorbing from the surface in the right side of Eq. (3.1) to an exponential over a range between 500–1000°C (also in GaN ML/s). Then Eq. (3.1) becomes:

$$\frac{1}{\tau_i} = \frac{1}{\tau_0} \exp\left(-\Delta H / k_B T_c\right) \qquad (3.3)$$

where ΔH is the enthalpy of vaporization of Ga and $1/\tau_0$ is an attempt frequency. Hence, at a given incoming Ga flux, the lowest possible surface temperature to avoid Ga condensation is given by:

$$T_c = \frac{\Delta H}{k_B \ln(\tau_i / \tau_0)} \qquad (3.4)$$

where ΔH is 2.71 eV, $\tau_0 = 4.43 \times 10^{-14}$ s/ML, and τ_i is the time it would take to form one ML of GaN on a (0001) plane assuming complete Ga incorporation. Thus, once the Ga source is calibrated, the surface temperature can be determined by finding the temperature at

which Ga condenses, using either RHEED or DMS.

It should be noted that each technique observes a different region of the surface. Depending on the collimation in our system DMS samples at least a 0.5 cm² region. The region sampled by RHEED depends on the spot size and incident angle—for a 0.1 mm spot and an incident angle of 2°, RHEED examines a stripe that is 0.1 mm by 6 mm. The latter could be used to map out the temperature gradient over the sample, but drift of the beam could also lead to variations in the measurements. Both methods are compared below.

The RHEED method is illustrated in Fig. 2. First one observes the RHEED intensity behavior above the condensation temperature as shown in Fig. 2a. The temperature is then reduced until Ga accumulation occurs as shown in Fig. 2c. The condensation temperature is then found by approaching the condition, from above and below, until a curve similar to Fig. 2b is obtained. The RHEED method was also applied to the case of In on GaN, assuming that the behavior is similar to that of Ga on GaN. The method does not work for Al on GaN, because such high temperatures are needed that GaN decomposes.

Alternatively, the condensation temperature can be found using DMS by monitoring the Ga flux desorbing from the sample. The desorbing Ga flux is monitored without NH_3 at an initially high surface temperature above Ga condensation. At such a temperature, the incoming flux equals the desorbing flux after steady state is reached. The surface temperature is then reduced until the desorbing flux starts to decrease from its initial constant maximum, indicating that Ga accumulates on the sample surface as shown in Fig. 6. The same procedure can be followed when there is an incident flux of NH_3—the difference is that the Ga signal will be reduced above the condensation temperature due to GaN formation. Nonetheless, the condensation temperature is clearly observed by a discontinuous change in slope as shown in the same figure. No GaN formation was detected below the condensation temperature for high Ga to NH_3 flux ratios, and the desorbing Ga flux decreases exponentially according to the Ga vapor pressure equation.

The results for both methods presented here are compiled in Fig. 7, which shows the offset from the thermocouple reading as a function of surface temperature for a typical sample mounting arrangement. Also shown are temperature offsets determined from the melting point of AlSi eutectics mounted on top of a GaN sample, as well as DMS and RHEED measurements using In. The AlSi eutectic temperature was observed by monitoring the temperature dependent emissivity with an IR pyrometer. All data points were taken on the same sample using the same mounting arrangement. Most data points fall within 20°C of a linear fit. Above 750°C, the data taken by a collimated DMS using Ga are reproducible to within 1°C. Below this temperature, low Ga fluxes are needed for the measurement and the signal-to-noise ratio is poor.

Note that the data above 750°C are in the range of typical GaN growth temperatures. The larger spread in the RHEED data is due to the combination of a temperature gradient across the sample of about 30° and fluctuations in beam position.

Growth Rate Measurements

Under GaN growth conditions of excess Ga (NH_3-limited growth) RHEED intensity oscillations were not observed[13] so that other *in situ* growth rate measurements are required. Using DMS, the difference between the incident and the desorbing Ga flux can be used to obtain the growth rate. This method, which does not require measurement of the sample area, is based on comparing the DMS signal with and without an NH_3 flux.

We consider deposition onto a surface at a temperature above which Ga condenses. A fraction of the incident Ga incorporates as GaN, and the remainder supplies a steady-state Ga surface concentration which desorbs at the same rate at which it is supplied. Without any NH_3 flux, all the incident Ga desorbs. We assume that an NH_3 flux does not affect the angular distribution of the desorbed Ga flux. In order to obtain the incorporating flux, we measure the difference between these two Ga desorption fluxes.

Examples of the Ga desorption signal with and without NH_3 are shown in Fig. 8 and were taken without collimation to improve the signal-to-noise ratio. Here we measure the change in the desorbed Ga signal when the Ga flux is interrupted since it is somewhat easier to be certain that steady state sig-
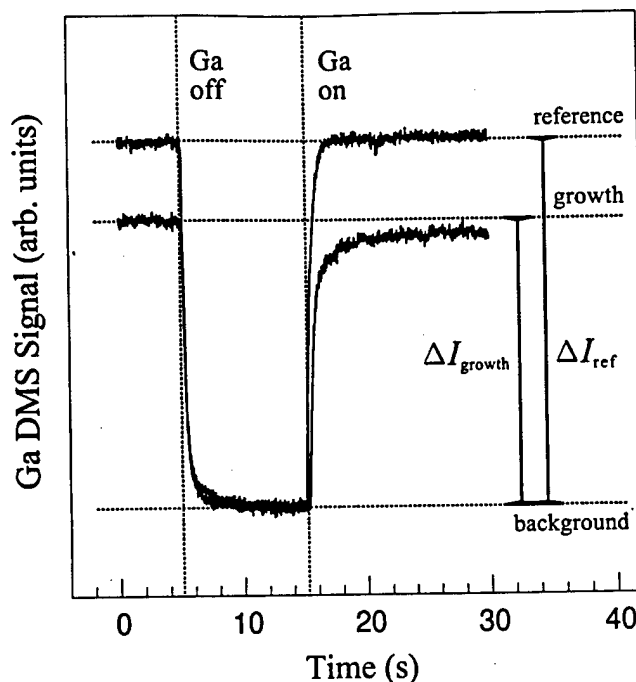

Fig. 8. Typical uncollimated Ga DMS signal during closing and opening of the Ga shutter. The growth and reference signal is obtained by measuring the rapid change in signal after closing the Ga shutter to avoid contributions of the slowly varying background signal from other cooler parts of the system. Growth rates are obtained by calculating the incorporation fraction from the signals and multiplying by the known incident flux. Note that the growth rate is obtained by closing the Ga shutter instead of opening to ensure steady state after 15 min of growth.
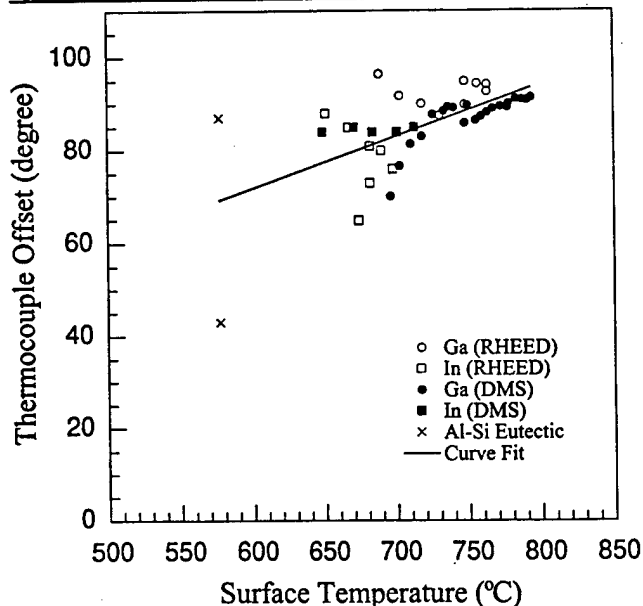

Fig. 7. The offset from the thermocouple reading determined as a function of surface temperature using Ga and In. Employing collimated Ga DMS the data were reproducible to within 1° at typical GaN growth temperatures. The spread in data for In DMS is due to the difficulties in calibrating the source, for Ga and In RHEED due to a temperature gradient across the sample, as well as low fluxes and slow desorption rates at low substrate temperatures. The validity of the method was verified employing the Al-Si eutectic. The large error is due to general problems with IR pyrometry in MBE environments.
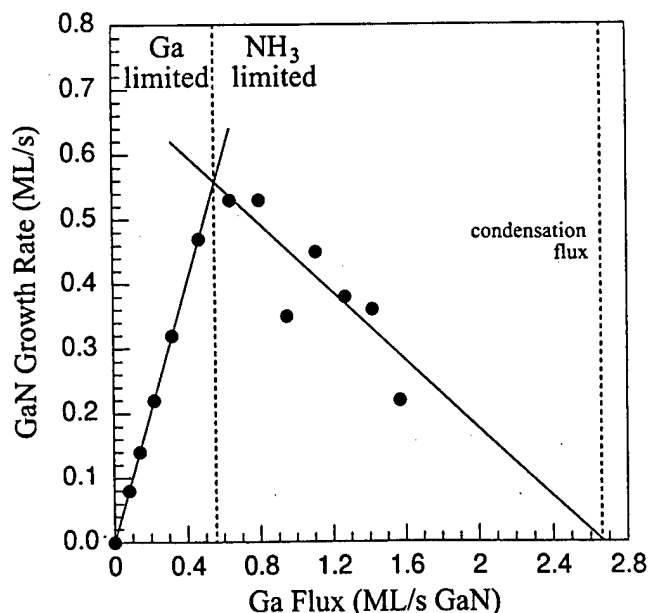

Fig. 9. GaN growth rate as a function of Ga flux at constant NH_3 BEP of 1×10^{-5} Torr and surface temperature of 785°C. Two growth regimes can be identified, Ga-limited and NH_3-limited. Near unity incorporation of Ga is obtained during Ga-limited growth. During NH_3-limited growth, the growth rate reduces as a function of Ga flux, approaching zero at the flux required for condensation at this temperature. This reduction is attributed to weakly adsorbed Ga blocking active Ga terminated GaN sites.
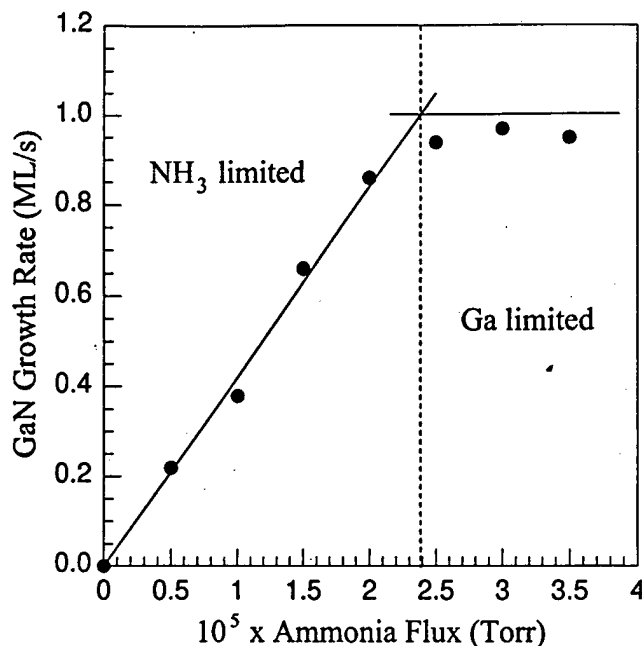
Fig. 10. GaN growth rate as a function of NH_3 flux at constant Ga flux of 1.0 ML/s (GaN) and surface temperature of 785°C. Both growth regimes can be identified, NH_3-limited and Ga-limited. In the NH_3-limited regime, the growth rate is a linear function of the NH_3 flux, while in the Ga-limited regime near unity Ga incorporation is obtained.
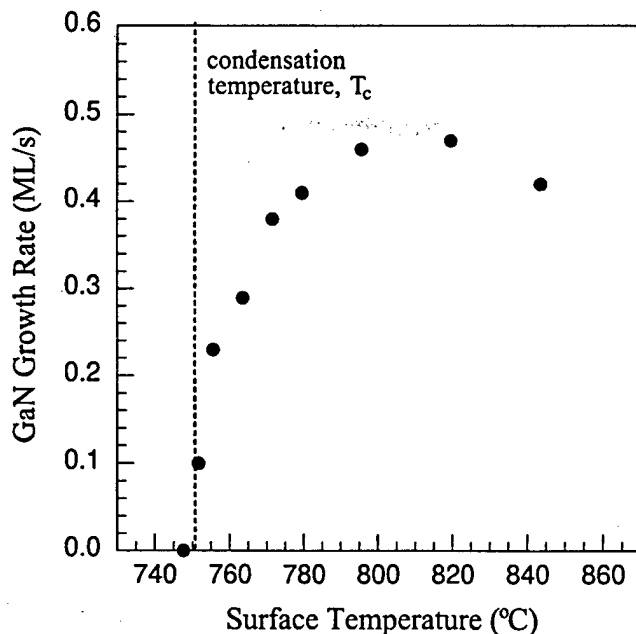

Fig. 11. GaN growth rate as a function of surface temperature at constant Ga flux of 1.0 ML/s (GaN) and NH_3 BEP of 1× 10⁻⁵ Torr. The growth rate reduces toward the condensation temperature, attributed to weakly adsorbed Ga blocking active Ga terminated GaN sites.
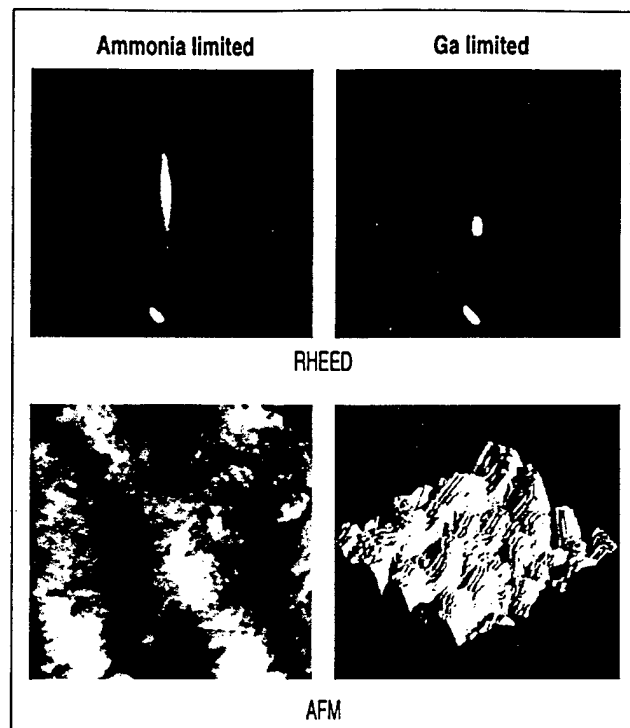

Fig. 12. RHEED patterns with the incident beam along the $\langle 1\bar{2}\bar{2}0 \rangle$ azimuth and AFM images for both NH_3 and Ga-limited growth. The AFM scans cover an area of 2 × 2 μm with a z-range of 50 and 1000Å, respectively. NH_3-limited growth gives rise to a weakly (2 × 2) reconstructed RHEED pattern (a) and AFM shows atomic steps on islands (c). Ga-limited growth results in a RHEED pattern with a strong transmission component (b) and AFM indicates that this is due to facets (d).

nals are measured. With NH_3 impinging on the surface, GaN is grown until steady state conditions are obtained, which in this case was about 15 min. The Ga flux is then interrupted and the DMS signal quickly decreases to a constant background level. We take the drop in the measured mass spectrometer current, ΔI_{growth}, to be proportional to the Ga flux leaving the

sample surface. Similarly, without NH_3, there is a drop in the Ga reference flux, ΔI_{ref}, that is proportional to the incident Ga flux. The growth rate is then computed from

$$\Gamma_{growth} = \frac{\Delta I_{ref} - \Delta I_{growth}}{\Delta I_{ref}} \cdot \Gamma_{in.} \qquad (3.5)$$

using Γ_{in} as measured by RHEED intensity oscillations and implicitly taking into account the proportionality factor between the measured mass spectrometer current and the desorption flux. Note that at substrate temperatures greater than about 800°C, the decomposition of GaN, not included in Eq. (3.5), must also be considered.

Using this method, Figs. 9, 10, and 11 show the GaN growth rate vs Ga flux, NH_3 flux, and substrate temperature, respectively. The DMS measurements were taken on the same sample, using a collimator to minimize the effect of the temperature gradient, with 15 min of GaN growth between the data points to ensure steady state conditions. Absolute growth rates calculated from the Ga signal were checked independently using a stylus and Rutherford backscattering spectroscopy.

From these three figures, a number of important conclusions about the MBE growth of GaN can be made. Figure 9 shows that the growth is Ga-limited

with near unity incorporation up to a certain Ga flux. At higher Ga fluxes, the growth rate is NH_3-limited and decreases with increased Ga flux, going to zero at the incident Ga flux that determines the condensation condition for this substrate temperature. We have attributed this reduction of growth rate to weakly adsorbed Ga that blocks active Ga terminated sites.[11,12] Figure 10 shows that the growth rate in the NH_3-limited regime is a linear function of the NH_3 flux, up to the flux where near unity Ga incorporation is obtained, beyond which the growth becomes Ga-limited. Growth rates as a function of substrate temperature are shown in Fig. 11. The growth rate decreases with decreasing substrate temperature going to zero at the condensation condition where multilayers of Ga cover the surface.

Surface Morphology

To characterize the surface morphology of GaN films grown under Ga and NH_3-limited growth conditions, we compared *in situ* RHEED during growth to atomic force microscopy (AFM) after growth in air. Under NH_3-limited growth, the weakly reconstructed (2×2) RHEED pattern indicates that the surface morphology has a 2-D component, shown in Fig. 12a. This is somewhat dependent on the buffer used to initiate growth on sapphire. During Ga-limited growth, the RHEED pattern has a strong transmission component, as seen in Fig. 12b. However, we could grow up to 15 layers of Ga-limited films yielding damped RHEED intensity oscillations. This was achieved by growing on a GaN surface previously prepared under NH_3-limited conditions. AFM measurements were conducted to correlate surface morphology with the RHEED results. NH_3-limited growth results in surfaces featuring atomic steps on micron sized islands with pinholes approximately 1000Å in diameter, while Ga-limited growth results in faceting, as shown in Fig. 12c and 12d. Preliminary studies indicate that NH_3-limited films grown close to the Ga-limiting transition have the smoothest surfaces.

SUMMARY

DMS and RHEED were used to find GaN surface temperatures by measuring the condensation temperature of Ga on Ga terminated GaN. For typical GaN growth temperatures of less than 800°C, the reproducibility of the method is better than 1° when using a collimated DMS. Further, RHEED was used to identify different surface compositions and coverages during GaN growth and post growth annealing. DMS was demonstrated to be an accurate, nondestructive, and fast method to determine growth rates over a wide range of GaN growth conditions for GaN MBE using NH_3. Finally, using these methods, two different GaN growth regimes have been identified— Ga-limited and NH_3-limited. It has been found that Ga-limited growth gives rise to faceting, resulting in a transmission RHEED pattern. On the other hand, NH_3-limited growth results in films featuring atomic steps and a weakly reconstructed (2×2) RHEED pattern.

REFERENCES

1. S. Strite, M.E. Lin and H. Morkoç, *Thin Solid Films* 231, 197 (1993).
2. A.M. Dabiran and P.I. Cohen, *J. Cryst. Growth* 150, 23 (1995).
3. W.S. Lee, G.W. Yoffe, D.G. Schlom and J.S. Harris, *J. Cryst. Growth* 111, 131 (1991).
4. Y. Moriyasu, H. Goto, N. Kuze and M. Matsui, *J. Cryst. Growth* 150, 916 (1995).
5. L.K. Li, Z. Yang and W.I. Wang, *Electron. Lett.* 31, 2127 (1995).
6. S. Nakamura, *Jpn. J. Appl. Phys.* Part 1, 30, 1620 (1991).
7. J.Y. Tsao, T.M. Brennan and B.E. Hammons, *Appl. Phys. Lett.* 53, 288 (1988).
8. C.R. Jones, T. Lei, R. Kaspi and K.R. Evans, *Proc. 1995 Fall MRS Mtg.*(Pittsburgh, PA: Mater. Res. Soc.).
9. F.A. Ponce, B.S. Krusor. J.S. Major, Jr., W.E. Plano and D.F. Welch, *Appl. Phys. Lett.* 67, 410 (1995).
10. B. Daudin. J.L. Rouviere and M. Arlery, *Appl. Phys. Lett.* 69, 2480 (1996).
11. D.E. Crawford, R. Held, A.M. Johnston, A.M. Dabiran and P.I. Cohen, *MRS Internet Journal of Nitride Semiconductor Research* 1, 12 (1996).
12. D.E. Crawford, Ph. D. Thesis, University of Minnesota, Minneapolis, MN.
13. A.M. Johnston, Ph.D. Thesis, University of Minnesota, Minneapolis, MN 55455.
14. *CRC Handbook of Chemistry and Physics,* 71st Ed., Editor-in-Chief David R. Lide, (Boca Raton: CRC Press, 1990), p. 5-70.

High barrier height GaN Schottky diodes: Pt/GaN and Pd/GaN

Lei Wang[a)] and M. I. Nathan

Department of Electrical Engineering, University of Minnesota, Minneapolis, Minnesota 55455

T-H. Lim

Department of Chemical Engineering and Material Science, University of Minnesota, Minneapolis, Minnesota 55455

M. A. Khan and Q. Chen

APA Optics Incorporated, 2950 N. E. 84th Lane, Blaine, Minnesota 55449

Platinum (Pt) and palladium (Pd) Schottky diodes on *n*-type GaN grown by metalorganic chemical vapor deposition were achieved and investigated. Aluminum was used for ohmic contacts. Barrier heights were determined to be as high as $\Phi_B = 1.13$ eV by the current–voltage (I–V) method and $\Phi_B = 1.27$ eV by the capacitance–voltage (C–V) method for the Pt/GaN diode, and $\Phi_B = 1.11$ eV, $\Phi_B = 0.96$ eV, and $\Phi_B = 1.24$ eV by I–V, activation energy (I–V–T), and C–V methods for the Pd/GaN diode, respectively. The ideality factors were obtained to be $n \sim 1.10$. © *1996 American Institute of Physics.* [S0003-6951(96)00909-8]

GaN is a promising semiconductor for high-temperature, high-frequency, and high-power device applications. The study of Schottky barrier contacts on GaN has great importance for these applications. Recently progress in material growth has been impressive and high quality GaN becomes available for such a study.

Schottky barrier contacts on GaN using gold (Au) have been reported.[1,2] According to the Schottky–Mott model, the barrier height equals the difference between metal work function and electron affinity of semiconductor χ (for GaN $\chi = 4.1$ eV).[3] The work functions of Pt, Pd, and Au are 5.65, 5.12, and 5.1 eV, respectively.[4] Pt and Pd are expected to form good Schottky contacts on GaN. Ohmic contacts on *n*-type GaN using aluminum (Al) have been reported in several papers.[1,2,5–7]

In this letter we report experimental results of Schottky barrier contacts on *n*-type GaN Pt and Pd. The GaN films used in this study were grown on sapphire using metalorganic chemical vapor deposition (MOCVD). The details of the growth and crystal properties have been previously reported.[8,9] The films were *n* type with thickness of about 4 μm, sheet resistance of about 1 KΩ/square, carrier concentration of about 10^{17} cm^{-3}, and Hall mobility of about 200 cm^2/V s at room temperature. The metals (about 3000 Å thick) were deposited via conventional electron-beam evaporation with base pressure up to 10^{-7} Torr. The Schottky and ohmic contact patterns with different dot sizes (diameters = 100, 200, and 400 μm on mask) were formed using photolithography and liftoff techniques. The distance between the adjacent Schottky and ohmic contact dots (from center to center) is about 650 μm. Before the evaporation, samples were dipped in diluted buffered oxide etch (BOE: H$_2$O = 1:10) for about 30 s to remove possible oxide on the surfaces. There were no annealing treatments conducted for all contacts.

Al was used for the ohmic contact. Without annealing treatment, Al/GaN contacts show good ohmic behavior. I–V

characteristics of a typical Al/GaN contact (measured from Al dot to Al dot) are shown in Fig. 1. The resistance is on the order of kiloohms and it is determined essentially by the sheet resistance of GaN. It is consistent with the calculation result of $R = L/(\mu_n NqS)$, where L is the length, S the area, μ_n the electron mobility, N the ionized donor density, and q the electron charge.

We used three methods to measure the barrier height: I–V, C–V, and activation energy (I–V–T).[10] I–V characteristics of Pt/GaN and Pd/GaN Schottky diodes are shown in Figs. 2 and 3(a). The leakage current density was generally less than 10^{-9} A/cm^2 at low bias voltage.

For thermionic emission and $V > 3kT/q$, the general diode equations are[11]

$$J = J_0 \exp(qV/nkT), \tag{1}$$

$$J_0 = A^* T^2 \exp(-\Phi_B/kT), \tag{2}$$

where J_0 is the saturation current density, n the ideality factor, k Boltzmann's constant, T the absolute temperature, A^* the effective Richardson coefficient, and Φ_B the barrier
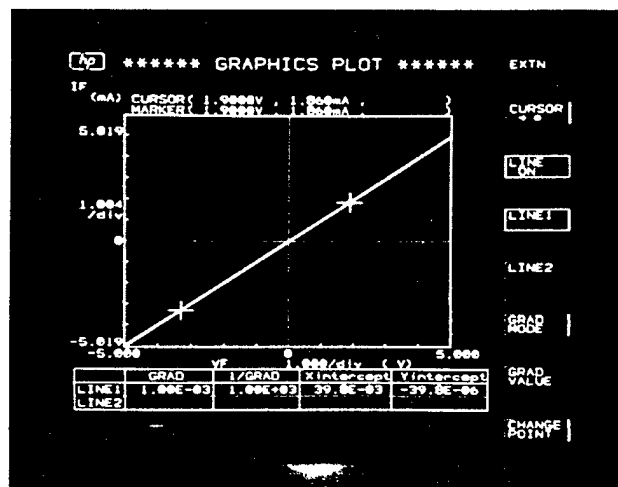

FIG. 1. *I*–*V* characteristics of Al/GaN ohmic contacts (measured from Al dot to Al dot, $S = 1.39 \times 10^{-3}$ cm^2).
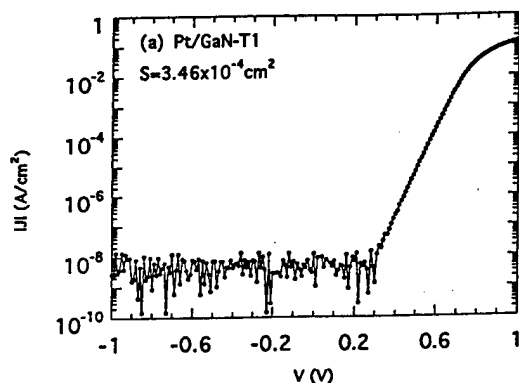
[a)]Electronic mail: leiwang@ee.umn.edu

FIG. 2. $I-V$ characteristics of Pt/GaN Schottky diodes. The measured contact area is 3.46×10^{-4} cm^2. I does not appear to be zero at $V=0$ because of noise.

height. J_0 can be obtained in the plot of $\log J$ vs V. J_0 $= 3.47 \times 10^{-13}$ A/cm^2 for Pt/GaN-T1 in Fig. 2 and J_0 $= 6.65 \times 10^{-13}$ A/cm^2 for Pd/GaN-D3 at room temperature. In the $I-V$ method Φ_B was determined from Eq. (2) at room temperature with theoretical value $A^* = 24$ A cm^{-2} K^{-2} [based on $A^* = 4\pi m^* q k^2/h^3$ and $m^* \approx 0.20 m_0$ (Ref. 12)], $\Phi_B = 1.13$ eV for Pt/GaN-T1 and $\Phi_B = 1.11$ eV for Pd/GaN-D3. In the $I-V-T$ method Φ_B and A^* were determined via a plot of $\ln(I_0/ST^2)$ vs $1/T$ (Fig. 3) based on Eq. (2), $\Phi_B = 0.96$ eV, and $A^* = 0.04$ A cm^{-2} K^{-2}. The measured
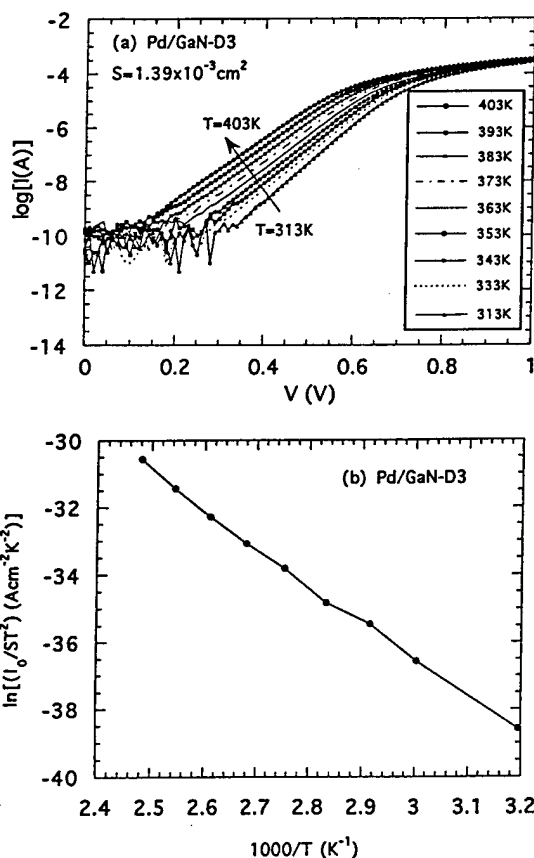

FIG. 3. Thermal activation energy method (Pd/GaN-D3). (a) $I-V$ characteristics at various temperatures. (b) Plot of $\ln(I_0/ST^2)$ vs $1/T$ with linear fit of $y = -3.19 - 11.11x$. $\Phi_B = 0.96$ eV and $A^* = 0.04$ A cm^{-2} K^{-2}.

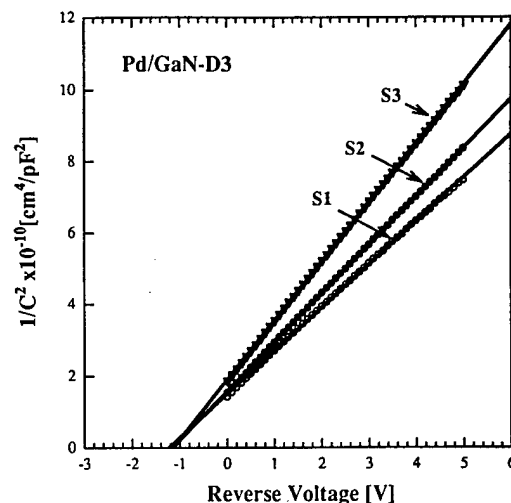

FIG. 4. $C-V$ characteristics of Pd/GaN-D3 Schottky diodes with three different contact areas ($S_1 = 9.50 \times 10^{-5}$ cm^2, $S_2 = 3.46 \times 10^{-4}$ cm^2, $S_3 = 1.39 \times 10^{-3}$ cm^2). $N \approx 1.11 \times 10^{17}$ cm^{-3}, $V_{bi} = 1.16$ V, and $\Phi_B = 1.24$ eV.

value of A^* is much smaller than the theoretical value. Hacke et al.[1] reported a measured value of $A^* = 0.006$ A cm^{-2} K^{-2} from Au/GaN.

$C-V$ measurements were performed at a frequency of 1 MHz. The $C-V$ relationship for a Schottky barrier is[11]

$$(1/C)^2 = (2/\epsilon q N S^2)(V_{bi} - V - kT/q),\qquad (3)$$

where ϵ is the permittivity (for GaN $\epsilon = 9.5\epsilon_0$).[12] $\Phi_B = q(V_{bi} + V_n)$, where $V_n = (kT/q)\ln(N_c/N)$, $N_c = 2.60 \times 10^{18}$ cm^{-3} based on $N_c = 2(2\pi m^* kT/h^2)^{3/2}$. From a measured plot of $1/C^2$ vs V (Fig. 4), $N \approx 1.11 \times 10^{17}$ cm^{-3}, $V_{bi} = 1.16$ V, and $\Phi_B = 1.24$ eV.

The results of barrier height, ideality factor, ionized donor density (from the Hall measurement), and breakdown voltage are summarized in Table I. The breakdown voltage was arbitrarily taken to be the voltage at which the reverse current exceeded 1 mA. It was found that Schottky contact (barrier height) relates to carrier concentration of GaN. If the carrier concentration is $\sim 10^{18}$ cm^{-3} or higher, the contact will be ohmic instead of Schottky contact. This is in agreement with the reported results of Au/GaN in which a good Schottky contact refers to $N = 6.6 \times 10^{16}$ cm^{-3},[1] and a leaky one with $N = 3 \times 10^{18}$ cm^{-3}.[2] The high carrier concentration might cause a tunneling effect at the interface. The barrier height of Au/GaN is close to the result of Hacke et al.[1] The

TABLE I. Summary of characteristics of GaN Schottky diodes.

| Diodes | Barrier height, Φ_B (eV) | | | Ideality factor, n | Carrier density (cm^{-3}) | Breakdown voltage (V) |
	$I-V$	$C-V$	$I-V-T$			
Pd/GaN-D1	1.11	1.24	—	1.20	9.4×10^{16}	-55
Pd/GaN-D2	1.05	1.30	—	1.02	1.4×10^{17}	-72
Pd/GaN-D3	1.11	1.24	0.96	1.09	1.2×10^{17}	-35
Pt/GaN-T1	1.13	1.27	—	1.10	9.4×10^{16}	-45
Pt/GaN-T2	0.89	1.12	—	1.05	1.2×10^{17}	-85
Pt/GaN-T3	0.52	—	—	2.96	4.3×10^{17}	-7
Au/GaN	0.88	—	—	1.06	7.0×10^{16}	-2

dependence of barrier height on the difference between the metal work function and the electron affinity of the semiconductor was not observed.

The values of the barrier height measured by the I–V method are always lower than those obtained by the C–V method in our measurements. This was also found in the GaAs (Au/GaAs) Schottky contact.[13] The reason might be partly due to the image-force barrier lowering effect.[10] The current distribution on the contact dots may not be uniform which can cause error in area S in the I–V method. The low Φ_B and small A^* found by the I–V–T method in one sample is a further suggestion of the possibility of nonuniform current distribution in the diodes.

In conclusion, good Schottky diodes on n-type GaN with Pt and Pd were achieved and investigated. Ohmic contacts were obtained using Al. Barrier heights were determined to be as high as $\Phi_B = 1.13$ eV by the I–V method and $\Phi_B = 1.27$ eV by the C–V method for the Pt/GaN diode, and $\Phi_B = 1.11$ eV, $\Phi_B = 0.96$ eV, and $\Phi_B = 1.24$ eV by I–V, I–V–T, and C–V methods for the Pd/GaN diode, respectively.

Since submission of this letter, study of the Schottky barrier on GaN using platinum (Pt) and palladium (Pd) has been reported by J. D. Guo et al. in Appl. Phys. Lett. **67**, 2657 (1995). They reported results similar to ours.

[1] P. Hacke, T. Detchprohm, K. Hiramatsu, and N. Sawaki, Appl. Phys. Lett. **63**, 2676 (1993).

[2] J. S. Foresi and T. D. Moustakas, Appl. Phys. Lett. **62**, 2859 (1993).

[3] J. I. Pankove and H. E. Schade, Appl. Phys. Lett. **25**, 53 (1974).

[4] H. B. Michaelson, in *CRC Handbook of Chemistry and Physics*, 75th ed., edited by D. R. Lide (CRC, Boca Raton, FL, 1994-1995), pp. 12–113.

[5] H. Amano, M. Kito, K. Hiramatsu, and I. Akasaki, Jpn. J. Appl. Phys. **28**, L2112 (1989).

[6] S. Nakamura, T. Mukai, and M. Senoh, Jpn. J. Appl. Phys. **30**, L1998 (1991).

[7] S. Nakamura, M. Senoh, and T. Mukai, Appl. Phys. Lett. **62**, 2390 (1993).

[8] M. Asif Khan, J. N. Kuznia, J. M. Van Hove, D. T. Olson, S. Krishnankutty, and R. M. Kolbas, Appl. Phys. Lett. **58**, 526 (1991).

[9] M. Asif Khan, J. M. Van Hove, J. N. Kuznia, and D. T. Olson, Appl. Phys. Lett. **58**, 2408 (1991).

[10] S. M. Sze, *Physics of Semiconductor Devices*, 2nd ed. (Wiley, New York, 1981).

[11] E. H. Rhoderick and R. H. Williams, *Metal-Semiconductor Contacts*, 2nd ed. (Clarendon, Oxford, 1988).

[12] A. S. Barker and M. Ilegems, Phys. Rev. B **7**, 743 (1973).

[13] F. A. Padovani and G. G. Sumner, J. Appl. Phys. **36**, 3744 (1965).

3 Publications and Talks

3.1 Publications

1. "Growth Rate Reduction Due to Surface Ga Accumulation," D. Crawford, R. Held, A.M. Johnston, A.M.Dabiran, and P.I. Cohen, MRS Internet Journal of Nitride Semiconductor Research, v1, (1996), no. 12.

2. "In Situ Control of GaN Growth by Molecular Beam Epitaxy," R. Held, D.E. Crawford, A.M. Johnston, A.M. Dabiran, and P.I. Cohen, J. Elect. Mater., v26 (1997) 272.

3. "N vs Ga limited growth of GaN," R. Held, D.E. Crawford, A.M. Johnston, and P.I. Cohen, in preparation, Surface Review and Letters, invited review.

4. "The sticking coefficient of Ga on GaN," in preparation.

5. A.M. Johnston, et al., "A comparison of supersonic jets sources," in preparation.

6. "High barrier height Schottky barriers on GaN", L. Wang, M.I. Nathan, Appl. Phys. Lett. v68 (1996) 1267.

3.2 Talks

1. "A comparison of ammonia and supersonic jets for the growth of GaN," A.M. Johnston, D.E. Crawford, R. Held, A.M. Dabiran, and P.I. Cohen, presented at the selected energy conference, JPL, Pasadena, 1995.

2. "N vs Ga limited growth of GaN," D. Crawford, R. Held, A.M. Johnston, A.M.Dabiran, and P.I. Cohen, Materials Research Society, Boston, Fall, 1996.

3. "In situ control of the growth of GaN using ammonia," R. Held, A.M. Johnston, D.E. Crawford, A.M. Dabiran, and P.I. Cohen, American Vacuum Society, Minneapolis, 1995.

4. "Growth Rate Reduction Due to Surface Ga Accumulation," D. Crawford, R. Held, A.M. Johnston, A.M.Dabiran, and P.I. Cohen, presented at the European Conference on wide bandgap semiconductors, EGW-1, 1996.

5. "Jet assisted incorporation of nitrogen," A.M. Johnston, D.E. Crawford, R. Held, A.M. Dabiran, and P.I. Cohen, presented at the selected energy conference, North Carolina, 1996.

6. "The effect of hydrostatic pressure on the electrical resistivity of n-type GaN and AlGaN films grown on sapphire to 12 kbars, " M.I. Nathan, P.P. Ruden, and P.I. Cohen, presented at the GaN Workshop, St. Louis, MO, 1993.

4 Ph.D. dissertations

1. Lei Wang, Ph.D., to be submitted, 1997, section entitled: "High barrier height Schottky barriers on GaN"

2. Devin Crawford: Ph.D. 1996, "The Effect of Growth Kinetics and Thermodynamics on the properties of GaN grown by MBE"

3. Andrew Johnston: Ph.D., 1996, "Molecular beam epitaxy of GaN"

Abstract: Johnston Dissertation

The recent advances in the performance of the blue, green and near ultraviolet optoelectronic devices grown on gallium nitride (GaN) have made GaN a commercially significant material. Future advances in these devices will depend in part on an improved understanding of the chemistry and kinetics of the growth of GaN. An improved understanding of the chemistry may make it possible to engineer the growth conditions so as to reduce the defect density and improve the device performance. The kinetics of the growth of GaN using ammonia in a molecular beam epitaxy (MBE) environment are investigated using in situ reflection high energy electron diffraction (RHEED) and desorption mass spectrometry (DMS) with ammonia, and energetic ammonia and molecular nitrogen supplied by jet sources. These experiments indicate that GaN dissociates with an activation energy of 3.4 ± 0.1 eV, that molecular nitrogen will dissociatively chemisorb on GaN with an activation energy of 6.7 ± 0.3 eV, that the ammonia dissociates on GaN in the presence of gallium with an activation energy of 0.66 ± 0.03 eV, and that the physisorption energy of molecular ammonia on GaN is approximately 0.09 ± 0.01 eV. Further, the ammonia chemisorbs to the GaN as NH2 and the physisorbed gallium inhibits the growth perhaps by occupying the sites for ammonia chemisorption. These results are discussed in terms of a simple growth model. Under ammonia-rich conditions strong RHEED intensity oscillations have been observed. A procedure for growing films of GaN on sapphire capable of producing RHEED oscillations is outlined. Finally, some initial experiments on the lattice matched substrate manganese oxide (MnO) are presented.

Abstract: Crawford Dissertation

The role of thermodynamic and kinetic processes in the growth of GaN by molecular beam epitaxy is investigated. A review of the thermodynamic properties of GaN as well as the other constituents in the growth system is presented. Due to a lack of existing experimental data, the Gibb's energy of GaN is estimated over a wide temperature range determining the heat capacity from chemical trends. The resulting temperature dependent entropy as calculated from this heat capacity combined with the third law of thermodynamics is in excellent agreement with published measurements of the Gibb's energy of formation of GaN at high temperature. This emperical approach enables extrapolation of these high temperature data to MBE growth conditions with a high degree of confidence.

Kinetic processes are examined during growth using reflection high energy electron diffraction (RHEED) and desorption mass spectroscopy (DMS). We find that the incorporation rate of ammonia during growth is reduced when excess Ga accumulates on the surface. In the absence of this accumulated Ga, ammonia incorporation is not kinetically limited for typical MBE conditions. Langmuir evaporation measurements of GaN are also reported and agree with previously published data for free Langmuir evaporation. When Ga flux is incident on the substrate surface, the decomposition rate decreases according to a mass-action law.

The buffer layer plays a key role in determining both the optical and electrical properties of the GaN films. Growth using a thin, low temperature AlN buffer layer leads to insulating films with reduced defect related luminesence. Films grown with thicker buffer layers at higher temperature are conducting and exhibit higher deep level luminesence intensity. Room temperature Hall mobilities in conducting films did not exceed 140 $cm^2V^{-1}s^{-1}$ with typical carrier concentrations of about $10^{18}cm^{-3}$.